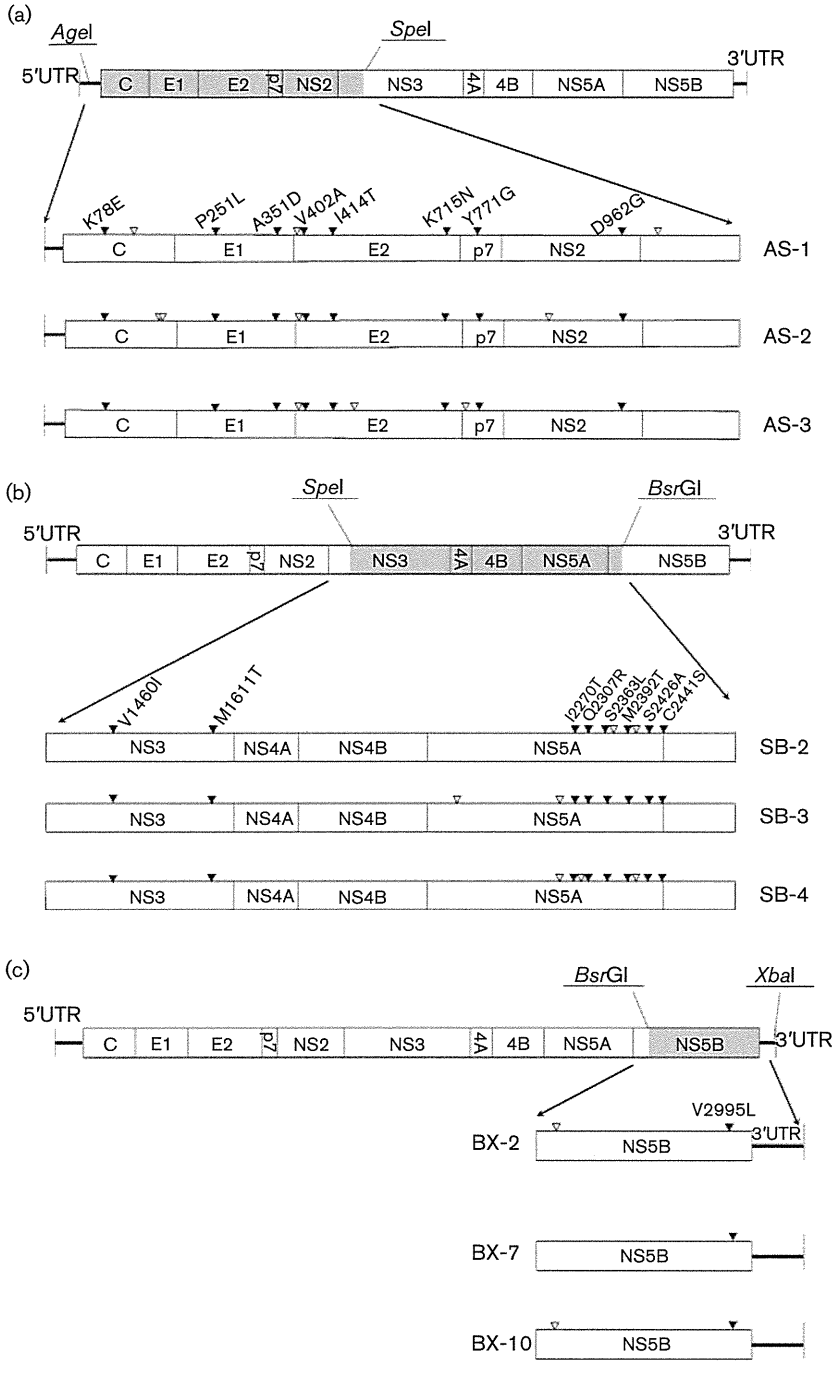

Fig. 1. Genetic mutations causing amino acid substitutions during long-term HCV infection. RT-PCR was performed for HCV RNAs from HuH-7 cells 130 days after JFH-1 infection. PCR products were subcloned into the pBluescript II plasmid. Three clones of (a) the Core to NS2 region between the *Age*I and *Spe*I sites (AS), (b) the NS3 to NS5A region between the *Spe*I and *Bsr*GI sites (SB) and (c) the NS5B to 3′X region between the *Bsr*GI and *Xba*I sites (BX) were subjected to sequencing analysis. ▼ and ▽ represent conservative and non-conservative amino acid substitutions, respectively.

Mutations in NS5B enhanced HCV RNA replication differently in genotypes 1b and 2a

V2995L in NS5B is a common substitution, occurring in three clones, and H2505Q is conserved in two clones (BX-2 and BX-10). We examined the corresponding amino acids at positions 2995 and 2505 in genotype 1b replication-competent HCV strains O, 1B-4 and KAH5 (Fig. 3a) (Nishimura *et al.*, 2009). The histidine at aa 2505 in JFH-1 is conserved in O, 1B-4 and KAH5 at the corresponding position, aa 2482. The valine at aa 2995 in JFH-1 is an alanine in O, 1B-4 and KAH5 at the corresponding position, aa 2972 (Fig. 3a). It is not clear whether the adaptive mutation found in genotype 2a is effective in genotype 1b HCV. Therefore, we investigated the effect of V2995L and/or H2505Q substitution on genotype 1b HCV RNA replication. We introduced substitutions V2995L and/or H2505Q into the subgenomic replicon, pOR/3-5B (HCV-O). In contrast to the case of JFH-1, H2505Q but not V2995L enhanced HCV-O RNA replication (Fig. 3b). These results indicate that the mutations in NS5B derived from JFH-1 functioned differently in genotype 1b HCV-O RNA replication.

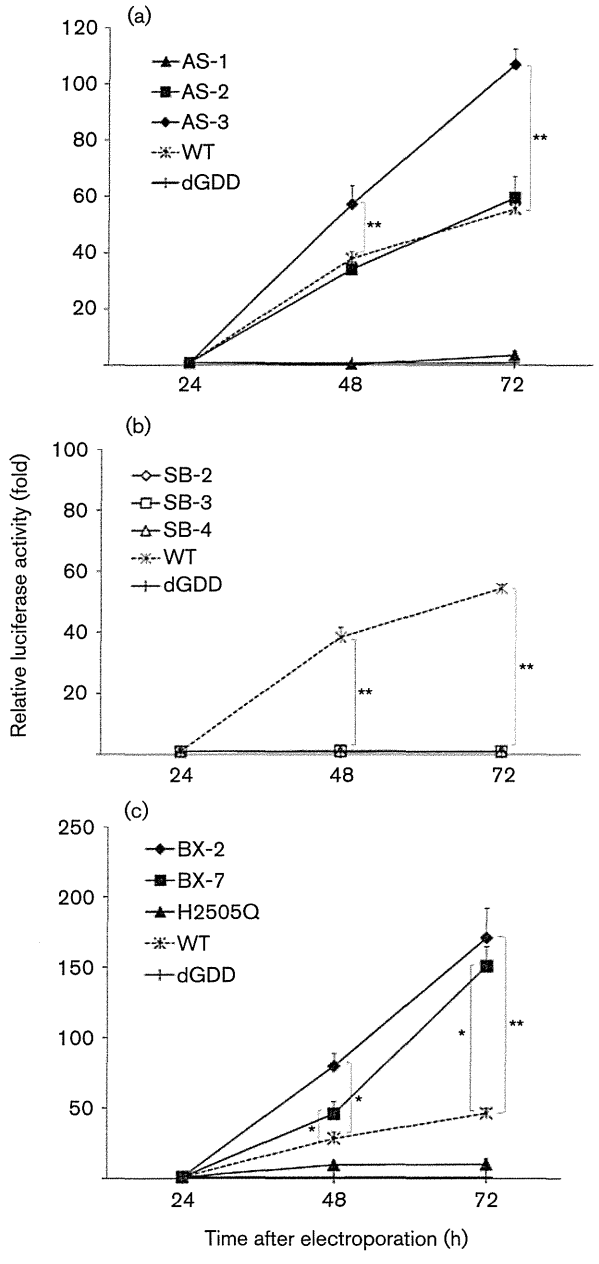

Fig. 2. Effect of amino acid substitutions on HCV RNA replication. (a) The Core to NS2 region; (b) the NS3 to NS5A region; (c) the NS5B to 3′X region. Amino acid substitutions were introduced into pJR/C5B and *in vitro*-synthesized RNAs were electroporated into HuH-7-derived RSc cells. RL activity was determined 24, 48 and 72 h after electroporation. dGDD, Negative control without the GDD motif; WT, wild type. *$P<0.05$; **$P<0.01$.

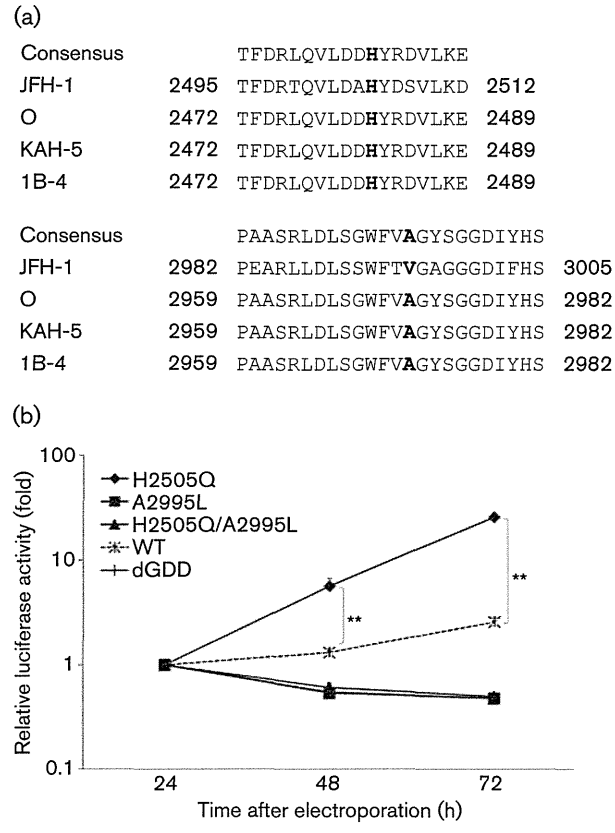

Fig. 3. Effect of amino acid substitutions in NS5B on genotype 1b and 2a HCV RNA replication. (a) Alignment of amino acids at positions 2505 (JFH-1) and 2482 (genotype 1b) and around the adjacent region (upper panel). Alignment of amino acids at positions 2995 (JFH-1) and 2972 (genotype 1b) and around the adjacent region (lower panel). The HCV strains O, KAH5 and 1B-4 belong to genotype 1b. (b) H2505Q and/or V2995L were introduced into the HCV-O subgenomic replicon (pOR/3-5B), and transcribed RNAs were electroporated into RSc cells. RL activities were tested 24, 48 and 72 h after infection. dGDD, Negative control without the GDD motif; WT, wild type. **$P<0.01$.

HCV infection in HuH-7- and Li23-derived cell lines

As well as viral genetic mutations, the choice of host cells is important for the efficiency of HCV RNA replication. Cured cells in which HCV RNAs were eliminated by IFN-α, such as HuH-7.5, HuH-7.5.1 and our RSc cells, exhibit higher replication efficiency than their parental HuH-7 cells (Ariumi *et al.*, 2007; Blight *et al.*, 2002; Zhong *et al.*, 2005). Therefore, we examined whether subcloned Li23 cells might enhance HCV RNA replication. We performed serial subcloning of Li23 cells from Li23-derived ORL8c cells by the limiting-dilution method (Fig. 4a). ORL8c cells are a cured cell line in which genome-length HCV RNAs were eliminated by interferon (IFN) treatment (Kato *et al.*, 2009). The subclonal Li23-derived cell lines were selected from among 50–100 independent single cells in 96-well plates by three-round limiting dilution from ORL8c cells (Fig. S1a, available in JGV Online). First, L8c15 cells were selected from their parental ORL8c cells by limiting dilution. Then, C22 cells were selected from their parental L8c15 cells by limiting dilution. Finally, D7 cells were selected from C22 cells by limiting dilution (Fig. S1b). Together, these steps resulted in the

selection of three subclonal cell lines that respectively exhibited the strongest replication efficiency in each round of selection. The lineages of the selected cell lines after three rounds of subcloning were designated L8c15, C22 and D7 cells, respectively.

We tested the subcloned cells for their HCV infectivities in comparison with those of HuH-7 and HuH-7-derived RSc cells. We reported previously that RSc cells could strongly support HCV replication and production (Kato *et al.*, 2009). Li23 and its derived ORL8c, L8c15, C22 and D7 cell lines were infected using the supernatant from RSc cells replicating JR/C-5B with BX-2 mutations at an m.o.i. of 0.2 (Fig. 4b, c). RL activities were determined 24, 48, 72 and 96 h after infection and f.f.u. ml^{-1} were determined 48 h after infection. The efficiency of HCV infectivity was highest in D7 cells, followed in order by C22, L8c15 and Li23 cells. HCV RNA replication in D7 cells was almost equal to that in RSc cells. These results suggest that the subcloned cell lines exhibit higher susceptibility to HCV infection than their parental cells.

Next, we further characterized the susceptibility of D7 cells to HCV infection in comparison with RSc cells, because D7 cells exhibited the highest susceptibility to HCV infection among the Li23-derived cell lines. D7 cells also exhibited the highest production and release of Core into the supernatant among the parental C22-derived subclonal

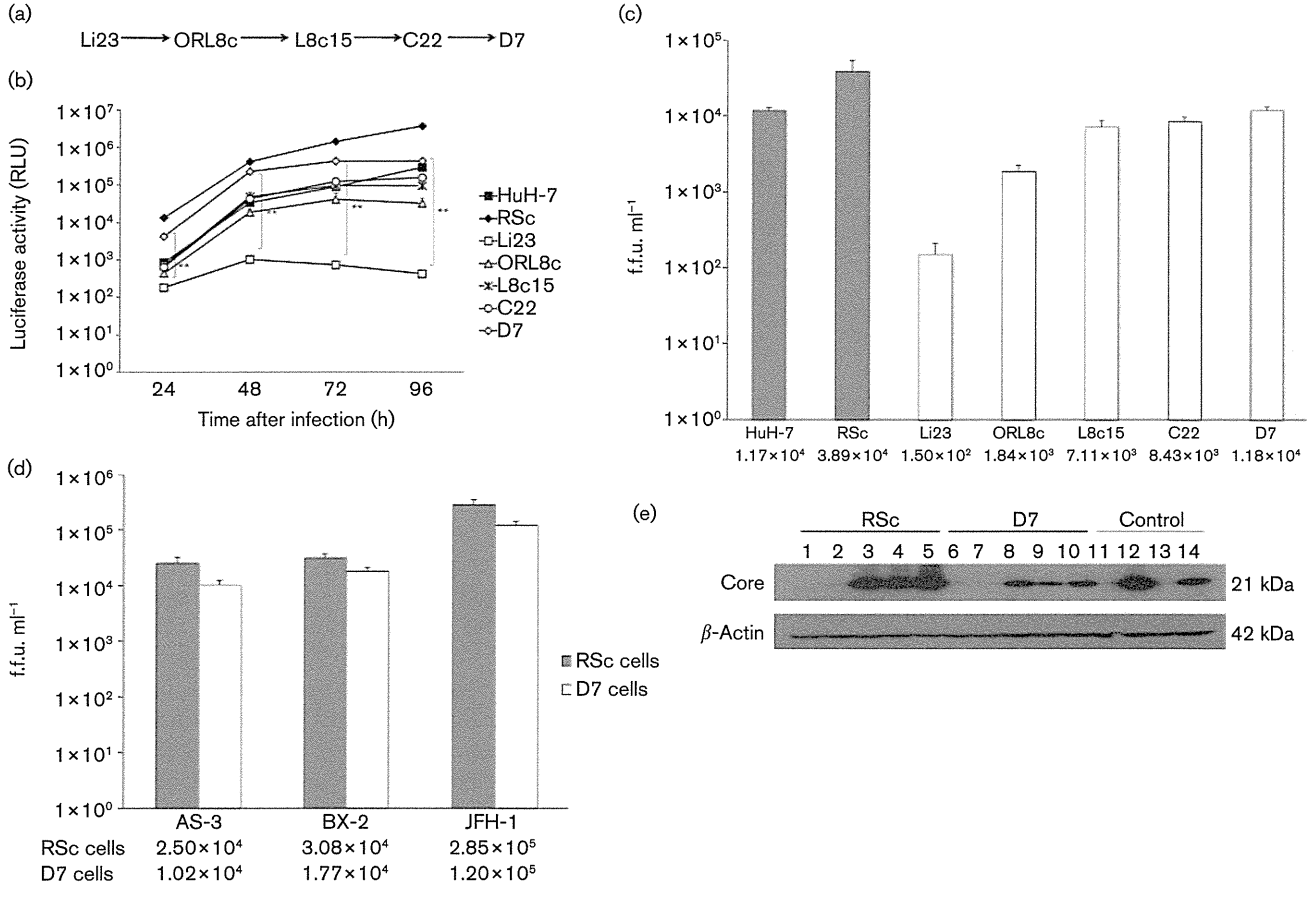

Fig. 4. HCV infection in HuH-7- and Li23-derived cell lines. (a) History of the selection of subclonal Li23-derived cell lines. (b) HuH-7, HuH-7-derived RSc, and Li23-derived ORL8c, L8c15, C22 and D7 cells were inoculated with supernatant from RSc cells replicating JR/C5B/BX-2. $^{**}P<0.01$. (c) f.f.u. ml^{-1} values were determined 48 h after infection of HuH-7- and Li23-derived cells with HCV using the supernatant from RSc cells replicating JR/C5B/BX-2 . (d) f.f.u. ml^{-1} values were determined 48 h after infection of RSc or D7 cells with HCV using the supernatant from RSc cells replicating JR/C5B/AS-3 or JR/C5B/BX-2. Supernatant from authentic JFH-1-replicating RSc cells was used as a positive control. (e) Core expression levels in RSc or D7 cells were determined 1, 2, 3 and 4 days after infection with JFH-1 with BX-2 mutations. Lanes: 1 and 6, mock-infected cells; 2 and 7, cells 1 day after infection; 3 and 8, cells 2 days after infection; 4 and 9, cells 3 days after infection; 5 and 10, cells 4 days after infection; 11 and 12, OR6c and OR6 cells, respectively; 13 and 14, ORL8c and ORL8 cells, respectively. OR6 and ORL8 were used as positive controls; OR6c and OR8c were used as negative controls. β-Actin was used as a control for the amount of protein loaded per lane.

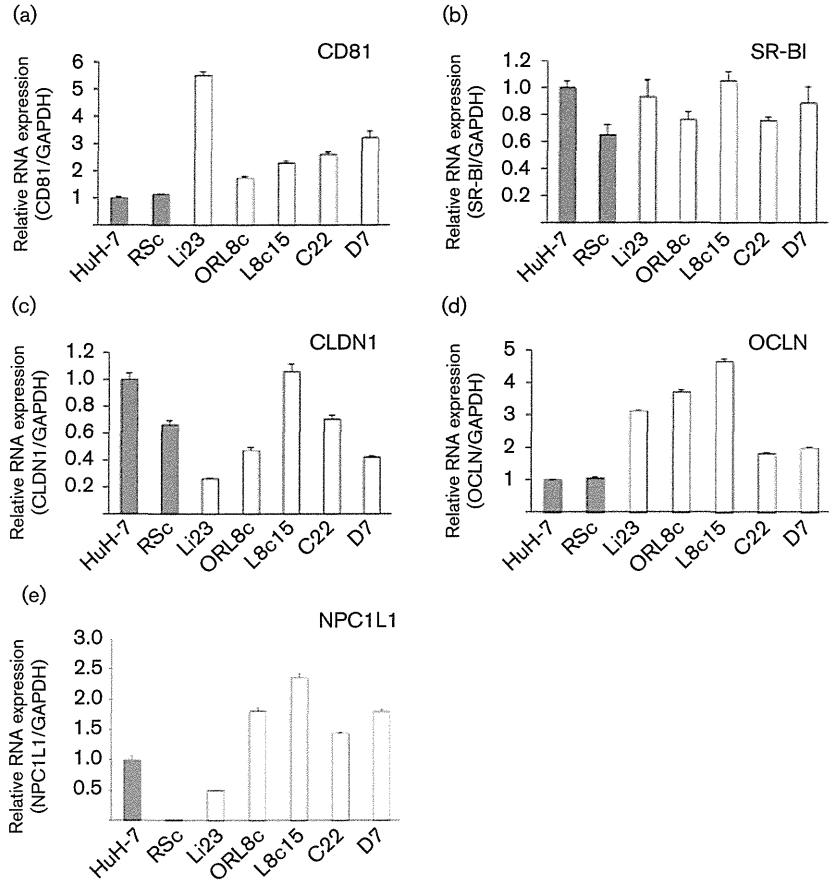

Fig. 5. Expression levels of HCV receptors in HuH-7- and Li23-derived cells. Quantitative RT-PCR was performed for CD81, SR-BI, CLDN1, OCLN and NPC1L1 as described in Methods. Relative expression levels of mRNA are shown, when the expression level of each receptor in HuH-7 was assigned to be 1. GAPDH was used as an internal control. Experiments were done in triplicate.

cells (Fig. S1b). The susceptibility of the HCV reporter-assay system to HCV infection was examined using HuH-7- and Li23-derived cells. Supernatants from RSc cells replicating JR/C-5B with AS-3 or BX-2 mutations were used as inocula. The supernatant from authentic JFH-1-replicating RSc cells was used as a positive control. RSc and D7 cells were inoculated with each HCV-containing supernatant and f.f.u. ml^{-1} were determined 48 h after infection. As shown in Fig. 4(d), the values of f.f.u. ml^{-1} for AS-3 were 2.5×10^4 and 1.0×10^4 in RSc and D7 cells, respectively; those for BX-2 were 3.1×10^4 and 1.8×10^4 in RSc and D7 cells, respectively; and those for authentic JFH-1 were 2.9×10^5 and 1.2×10^5 in RSc and D7 cells, respectively. These results indicate that the infectivities of these three inocula were almost equal in RSc and D7 cells.

Next we examined Core expression after infection of RSc and D7 cells with HCV, as D7 cells exhibited the highest infectivity among the Li23-derived cell lines (Fig. 4e). Core was detected 2, 3 and 4 days after infection of the supernatant from RSc cells infected by JR/C-5B with BX-2. Although Core expression in D7 cells was slightly weaker than that in RSc cells, the signal of Core in HCV-infected D7 cells was equal to that in stable ORL8 cells. These results suggest that the JFH-1 reporter-assay system in Li23 cells is useful not only for the RL assay, but also for Core expression.

Expression of HCV receptors in parental and subclonal hepatoma cell lines

We tested expression of the HCV receptors CD81, scavenger receptor class B member I (SR-BI), claudin-1 (CLDN1) and occludin (OCLN). We also examined the expression of the recently reported HCV entry factor Niemann–Pick C1-like 1 (NPC1L1) (Sainz *et al.*, 2012). Expression levels of CD81 in Li23 and its subclonal cells were higher than those in HuH-7 and RSc cells (Fig. 5a). Although expression of CD81 in Li23-derived cell lines was lower than that in parental Li23 cells, interestingly the expression levels of CD81 increased during the rounds of selection. There is no difference in the expression of SR-BI among the cell lines tested (Fig. 5b). The expression of CLDN1 in Li23-derived cells was higher than that in parental Li23 cells (Fig. 5c). Expression levels of OCLN in Li23 and its subclonal cells were higher than those in HuH-7 and RSc cells (Fig. 5d). Finally, the expression of NPC1L1 in Li23-derived cell lines was higher than that in parental Li23 cells (Fig. 5e). It is noteworthy that the expression level of NPC1L1 in RSc cells was approximately 2 $\log_{10}$ lower than that in parental HuH-7 cells. Taken together, these results indicate that the expression levels of CLDN1 and NPC1L1 in Li23-derived cells were higher than those in parental Li23 cells.

Life cycle of the HCV reporter-assay system in Li23-derived cells

We investigated whether D7 cells produce infectious HCV. First, D7 cells were inoculated using the supernatant from RSc cells replicating JR/C5B with BX-2, and the supernatant was stored at 17 days after infection. Then, the supernatant derived from the D7 cells was used as an inoculum for reinfection of naïve D7 cells. RL activities were determined 2, 6, 10 and 14 days after reinfection (Fig. 6). RL activity was increased after reinfection in D7 cells and reached a plateau 10 days after reinfection. These data indicate that the JFH-1 reporter-assay system is also useful for monitoring the HCV life cycle in Li23-derived cell lines.

DISCUSSION

In this study, we developed an HCV production reporter-assay system using two distinct hepatoma cell lines, HuH-7 and Li23. Robust HCV RNA replication and virus production were achieved by the introduction of REMs into the structural region or the NS5B region. These REMs were obtained from JFH-1-infected long-term-cultured cells. The two REMs in NS5B (H2505Q and V2995L substitutions) derived from JFH-1 had different effects on replication of genotype 1b HCV-O RNA and genotype 2a JFH-1 RNA. Furthermore, the subcloned Li23-derived D7 cells produced by serial limiting dilution supported this HCV production reporter-assay system.

Several groups have reported JFH-1 reporter virus systems (Koutsoudakis *et al.*, 2006; Marcello *et al.*, 2006; Pietschmann *et al.*, 2002; Wakita *et al.*, 2005). However, robust reporter virus production was limited within the study using HuH-7-derived cells. Therefore, we attempted to developed a JFH-1 reporter virus assay system using our previously reported line of Li23 cells (Kato *et al.*, 2009).

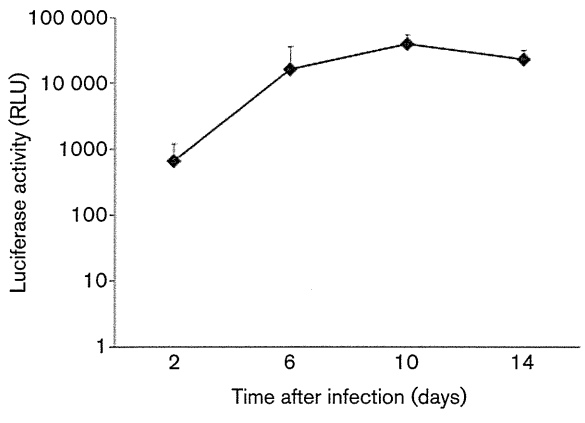

Fig. 6. HCV life cycle in Li23-derived D7 cells. D7 cells were inoculated with the supernatant from D7 cells after infection with JFH-1 with BX-2 mutants. RL activities were tested 2, 6, 10 and 14 days after infection.

The introduction of RL and EMCV-IRES genes into the HCV gene lengthened the genome of HCV by approximately 1.9 kb and led to a reduction in the efficiency of HCV RNA replication. To overcome this disadvantage, we adopted the following strategies: (i) introduce the REMs; (ii) select cloned Li23-derived cells with a highly permissive host condition by the serial limiting-dilution method. For the first purpose, we performed sequence analyses for HCV RNA from JFH-1-infected RSc cells. Mutations in the region from Core to NS2 or NS5B enhanced HCV RNA replication. However, combination of mutations from two different regions reduced HCV RNA replication (Fig. S2). The reason for this may be that these two mutation clusters were obtained from distinct RT-PCR-amplified clones and they were not necessarily located on the same viral genome. It has been reported that the combination of REMs exhibited an antagonistic effect on HCV RNA replication (Lohmann *et al.*, 2001). For the second purpose, we selected highly permissive Li23-derived clonal cells by the limiting-dilution method. We obtained three Li23-derived subclonal cell lines, L8c15, C22 and D7, in order from parental Li23-derived ORL8c cells. The efficiency of infectivity was highest in D7 cells, followed in order by C22, L8c15 and Li23 cells. D7 cells were highly permissive for infection of HCV with NS5B mutations.

As shown in Fig. 3(a), the histidine at aa 2505 in JFH-1 was conserved in the replication-competent O, 1B-4 and KAH5 strains at the corresponding position, aa 2482. The valine at aa 2995 in JFH-1 was alanine in strains O, 1B-4 and KAH5 at the corresponding position, aa 2972. The REMs in genotype 1b HCV were usually obtained by selection with neomycin after HCV RNA electroporation. Pietschmann *et al.* (2009) reported that REMs impaired infectious virus production. Most REMs are located in the NS3 and NS5A regions (Abe *et al.*, 2007; Blight *et al.*, 2002; Lohmann *et al.*, 2001; Pietschmann *et al.*, 2002). NS5A is a key molecule for virus production, and REMs affect the phosphorylation status of NS5A and the interaction with Core (Kato *et al.*, 2008; Masaki *et al.*, 2008; Tellinghuisen *et al.*, 2008). In contrast, our REMs in NS5B were obtained in JFH-1-infected long-term cell culture without drug selection. Taking this information into account, we considered that H2505Q in NS5B might not interfere with genotype 1b virus production. We attempted to apply this REM from genotype 2a to genotype 1b and found that H2505Q enhanced replication of the genotype 1b HCV-O replicon. We are currently investigating whether our NS5B REM could enhance genotype 1b HCV production. As for the substitution at aa 2995 in JFH-1 (aa 2972 in genotype 1b), we should be careful in interpretation, because the backgrounds at this position are different between genotypes 2 and 1. Analysis of an HCV database (http://s2as02.genes.nig.ac.jp/) revealed that the consensus amino acids at position 2995 in genotype 2 and at 2972 in genotype 1 were valine and alanine, respectively. Furthermore, alanine and valine are not found at position 2995 in genotype 2 or at 2972 in genotype 1, respectively. These observations

indicate that amino acid substitution between alanine and valine at these positions may be lethal for HCV of both genotypes. The amino acid at position 2995 in genotype 2 (2972 in genotype 1) is just upstream of a *cis*-acting replication element in NS5B. Therefore, the nucleotide at this position may affect the HCV RNA replication. To clarify this issue, further study will be needed.

A comparative study using HuH-7- and Li23-based JFH-1 reporter-assay systems would be expected to reveal new information on virus entry and release steps, because the backgrounds of these cells are different. Our recent study of these cells revealed the difference in sensitivities to anti-HCV reagents including ribavirin and methotrexate (Mori *et al.*, 2011; Ueda *et al.*, 2011). Furthermore, the IL28B genotype was different between HuH-7 and Li23 cells. The IL28B genotype (rs8099917) of HuH-7 cells renders them resistant to pegylated IFN and ribavirin, and Li23 cells are sensitive to pegylated IFN and ribavirin (M. Ikeda and N. Kato, unpublished data).

Recently, it was reported that stable expression of miR122 enhanced JFH-1 HCV production in Hep3B and HepG2 (Kambara et al., 2012; Narbus et al., 2011). It is noteworthy that the expression of miR122 in Li23-derived cells was almost the same as that in HuH-7 cells (Fig. S3). High-level expression of miR122 in Li23 cells may be one of the reasons that Li23 cells can support HCV production as robust as that in HuH-7 cells among the hepatocyte-derived cell lines. Interestingly, the expression levels of miR122 are higher in ORL8c, L8c15 and D7 cells, but not in C22 cells, than those in parental Li23 cells (Fig. S3). This result suggests that the expression level of miR122 may partly contribute to the fitness of HCV replication and production.

So far, we have only little information regarding the mechanism by which subclonal cells support HCV replication and production more efficiently than the parental cells. In this study, we found that the expression levels of CLDN1 and NPC1L1 in Li23-derived subclonal cells were higher than those in the parental Li23 cells. These results suggest that a high expression level of these entry factors in Li23-derived subclonal cells may contribute to enhanced virus entry. In the course of the experiment to determine the expression levels of NPC1L1 in HuH-7- and Li23-derived cell lines, we found that RSc cells expressed a very low level of NPC1L1 compared with the parental HuH-7 cells. Possible mechanisms for this are: (i) very low-level expression of NPC1L1 is sufficient for HCV entry; (ii) an unknown entry factor compensates for NPC1L1 in the entry step in RSc cells. Further study will be needed to clarify this issue.

In summary, we have developed JHF-1 reporter-assay systems using HuH-7-derived RSc and Li23-derived D7 cells. Expression levels of CLDN1 and NP1C1L were higher than those in the parental Li23 cells. We found different effects of REMs (V2995L and H2505Q) in NS5B on virus RNA replication in genotype 2a and 1b HCV strains. These findings will become useful tools for the study of the life cycle of HCV.

METHODS

Cell cultures. RSc and ORL8c cells were derived from the cell lines HuH-7 and Li23, respectively, as described previously (Kato *et al.*, 2009). L8c15, D7 and C22 cells were selected from ORL8c, L8c15 and C22 cells, respectively, by limiting dilution. HuH-7 and RSc cells were cultured in Dulbecco's modified Eagle's medium (DMEM; Life Technologies) supplemented with 10 % FBS (Life Technologies). Li23-derived cell lines were maintained in F12 medium (Life Technologies) and DMEM (1 : 1 in volume) supplemented with 1 % FBS and epidermal growth factor (50 ng ml^{-1}; PeproTech, Inc.) as described previously (Kato *et al.*, 2009).

RT-PCR and sequencing analysis. RSc cells were infected with cell-culture-grown HCV (HCVcc) and cultured for 130 days. Total RNAs from these cells were prepared using an RNeasy extraction kit (Qiagen). These RNA samples were used for RT-PCR in order to amplify the Core to NS2 (4.0 kb), NS3 to NS5A (3.6 kb) and NS5B to 3′X (1.9 kb) regions. Reverse transcription was performed with an oligo$(dA)_{23}$ primer. The following primer pairs were employed: to amplify the Core to NS2 region, JFH-1/*AgeI* (5′-CCCAAGCTTAC-CGGTGAGTACACCGGAATTGC-3′) and JFH-1/*Spe*IR (5′-TGCCA-TGTGCCTTGGATAGGTACG-3′); for the NS3 to NS5A region, JFH-1/*Spe*I (5′-CCCAGGGGTACAAAGTACTAGTGC-3′) and JFH-1/*Bsr*GIR (5′-CCCAAGCTTTACCTTTTTAGCCCTCTGTGAGGC-3′); for the NS5B to 3′X region, JFH-1/*Bsr*GI (5′-CCGCTCGAGACCC-TTTGAGTAACTCGCTGTTGC-3′) and JFH-1/*Xba*IR (5′-GCTCTA-GACATGATCTGCAGAGAGACCAGTTAC-3′). SuperScript III reverse transcriptase (Invitrogen) and KOD-plus DNA polymerase (TOYOBO) were used for reverse transcription and PCR, respectively. PCR products were ligated into pBluescript II (Fermentas) and three independent clones were subjected to sequencing analysis.

Plasmid construction. pJR/C-5B plasmid is a dicistronic HCV JFH-1 construct. The RL gene and HCV ORF were introduced into the first and second cistrons, respectively. To construct this plasmid, we fused the JFH-1 5′UTR with the RL gene by overlap PCR, and the PCR products were ligated into pFGR-JFH-1 (GenBank accession no. AB237837) at the *AgeI* and *PmeI* sites. For the first PCR, the primer pair 5′-GCGCCTAGCCATGGCGTTAGTATG-3′ (J5dC) and 5′-AAGCCATGGCCGGCCCTGGGCGACGGTTGGTGTTTCTTTTGG-3′ (J5dCR) was employed to amplify the 5′UTR, and the primer pair 5′-AACCGTCGCCCAGGGCCGGCCATGGCTTCCAAGGTGTACG-ACCCC-3′ (JRL) and 5′-TCGAAATCTCGTGATGGCAGGTTGG-3′ (JRLR) was employed to amplify the RL region. These first PCR products were used in the second PCR as the templates. For the second PCR, the primer pair J5dC and JRLR was employed to amplify the 5′UTR and RL. KOD-plus DNA polymerase was used for PCR.

The H2505H and/or A2995L mutations were introduced into the HCV-O replicon by QuikChange mutagenesis (Stratagene) as described previously (Ikeda *et al.*, 2002).

Luciferase reporter assay. For the luciferase assay, approximately $1.0–1.5 \times 10^4$ HCV-harbouring cells were plated onto 24-well plates in triplicate and were cultured for 24–96 h after electroporation or infection, as described previously (Ikeda *et al.*, 2005). The cells were harvested with *Renilla* lysis reagent (Promega) and subjected to RL assay according to the manufacturer's protocol.

Western blot analysis. Preparation of cell lysates, SDS-PAGE and immunoblotting were performed as described previously (Kato *et al.*, 2003). The antibodies used in this study were Core (CP11; Institute of Immunology, Tokyo, Japan) and β-actin (AC-15; Sigma) antibodies. Immunocomplexes were detected with a Renaissance enhanced chemiluminescence assay (PerkinElmer Life Science).

HCV infection and determination of f.f.u. To determine f.f.u. ml^{-1}, 6×10^3 cells were plated onto a 96-well plate 24 h before infection. The supernatant of HCV RNA-replicating cells was diluted serially and was used as an inoculum. Forty-eight hours after infection, the cells were fixed and Core was stained with anti-Core antibody and HRP-conjugated mouse anti-IgG antibody. Then, the expression of Core was visualized with a DAB substrate kit (DAKO). Culture supernatants and cells were collected for quantification of Core by ELISA (Mitsubishi Kagaku Bio-Clinical Laboratories).

Quantitative RT-PCR analysis. Quantitative RT-PCR analysis for HCV receptors was performed using real-time LightCycle PCR (Roche Diagnostics) as described previously (Ikeda *et al.*, 2005). The primer pairs for CD81, SR-BI, CLDN1 and OCLN were reported previously (Nakamuta *et al.*, 2011). The primer pair NPC1L1 (5′-AGATCTTCTTCTTCCGCCTCCA-3′) and NPC1L1R (5′-TGCCAG-AGCCGGGTTAAC-3′) was used for NPC1L1.

Statistical analysis. Luciferase activities were compared statistically between the various treatment groups using Student's *t*-test. *P*-values of <0.05 were considered statistically significant. The mean $\pm$ SD was determined from at least three independent experiments.

ACKNOWLEDGEMENTS

The authors would like to thank Masayo Takemoto, Takashi Nakamura and Keiko Takeshita for their technical assistance. This work was supported by Grants-in-Aid for Research on Hepatitis from the Ministry of Health, Labour, and Welfare of Japan.

REFERENCES

Abe, K., Ikeda, M., Dansako, H., Naka, K. & Kato, N. (2007). Cell culture-adaptive NS3 mutations required for the robust replication of genome-length hepatitis C virus RNA. *Virus Res* **125**, 88–97.

Ariumi, Y., Kuroki, M., Abe, K., Dansako, H., Ikeda, M., Wakita, T. & Kato, N. (2007). DDX3 DEAD-box RNA helicase is required for hepatitis C virus RNA replication. *J Virol* **81**, 13922–13926.

Blight, K. J., McKeating, J. A. & Rice, C. M. (2002). Highly permissive cell lines for subgenomic and genomic hepatitis C virus RNA replication. *J Virol* **76**, 13001–13014.

Ikeda, M., Yi, M., Li, K. & Lemon, S. M. (2002). Selectable subgenomic and genome-length dicistronic RNAs derived from an infectious molecular clone of the HCV-N strain of hepatitis C virus replicate efficiently in cultured Huh7 cells. *J Virol* **76**, 2997–3006.

Ikeda, M., Abe, K., Dansako, H., Nakamura, T., Naka, K. & Kato, N. (2005). Efficient replication of a full-length hepatitis C virus genome, strain O, in cell culture, and development of a luciferase reporter system. *Biochem Biophys Res Commun* **329**, 1350–1359.

Kambara, H., Fukuhara, T., Shiokawa, M., Ono, C., Ohara, Y., Kamitani, W. & Matsuura, Y. (2012). Establishment of a novel permissive cell line for the propagation of hepatitis C virus by expression of microRNA miR122. *J Virol* **86**, 1382–1393.

Kato, N. (2001). Molecular virology of hepatitis C virus. *Acta Med Okayama* **55**, 133–159.

Kato, N., Hijikata, M., Ootsuyama, Y., Nakagawa, M., Ohkoshi, S., Sugimura, T. & Shimotohno, K. (1990). Molecular cloning of the human hepatitis C virus genome from Japanese patients with non-A, non-B hepatitis. *Proc Natl Acad Sci U S A* **87**, 9524–9528.

Kato, N., Sugiyama, K., Namba, K., Dansako, H., Nakamura, T., Takami, M., Naka, K., Nozaki, A. & Shimotohno, K. (2003). Establishment of a hepatitis C virus subgenomic replicon derived from human hepatocytes infected in vitro. *Biochem Biophys Res Commun* **306**, 756–766.

Kato, T., Choi, Y., Elmowalid, G., Sapp, R. K., Barth, H., Furusaka, A., Mishiro, S., Wakita, T., Krawczynski, K. & Liang, T. J. (2008). Hepatitis C virus JFH-1 strain infection in chimpanzees is associated with low pathogenicity and emergence of an adaptive mutation. *Hepatology* **48**, 732–740.

Kato, N., Mori, K., Abe, K., Dansako, H., Kuroki, M., Ariumi, Y., Wakita, T. & Ikeda, M. (2009). Efficient replication systems for hepatitis C virus using a new human hepatoma cell line. *Virus Res* **146**, 41–50.

Koutsoudakis, G., Kaul, A., Steinmann, E., Kallis, S., Lohmann, V., Pietschmann, T. & Bartenschlager, R. (2006). Characterization of the early steps of hepatitis C virus infection by using luciferase reporter viruses. *J Virol* **80**, 5308–5320.

Lindenbach, B. D., Evans, M. J., Syder, A. J., Wölk, B., Tellinghuisen, T. L., Liu, C. C., Maruyama, T., Hynes, R. O., Burton, D. R. & other authors (2005). Complete replication of hepatitis C virus in cell culture. *Science* **309**, 623–626.

Lohmann, V., Körner, F., Koch, J., Herian, U., Theilmann, L. & Bartenschlager, R. (1999). Replication of subgenomic hepatitis C virus RNAs in a hepatoma cell line. *Science* **285**, 110–113.

Lohmann, V., Körner, F., Dobierzewska, A. & Bartenschlager, R. (2001). Mutations in hepatitis C virus RNAs conferring cell culture adaptation. *J Virol* **75**, 1437–1449.

Marcello, T., Grakoui, A., Barba-Spaeth, G., Machlin, E. S., Kotenko, S. V., MacDonald, M. R. & Rice, C. M. (2006). Interferons α and λ inhibit hepatitis C virus replication with distinct signal transduction and gene regulation kinetics. *Gastroenterology* **131**, 1887–1898.

Masaki, T., Suzuki, R., Murakami, K., Aizaki, H., Ishii, K., Murayama, A., Date, T., Matsuura, Y., Miyamura, T. & other authors (2008). Interaction of hepatitis C virus nonstructural protein 5A with core protein is critical for the production of infectious virus particles. *J Virol* **82**, 7964–7976.

Mori, K., Ikeda, M., Ariumi, Y. & Kato, N. (2010). Gene expression profile of Li23, a new human hepatoma cell line that enables robust hepatitis C virus replication: comparison with HuH-7 and other hepatic cell lines. *Hepatol Res* **40**, 1248–1253.

Mori, K., Ikeda, M., Ariumi, Y., Dansako, H., Wakita, T. & Kato, N. (2011). Mechanism of action of ribavirin in a novel hepatitis C virus replication cell system. *Virus Res* **157**, 61–70.

Narbus, C. M., Israelow, B., Sourisseau, M., Michta, M. L., Hopcraft, S. E., Zeiner, G. M. & Evans, M. J. (2011). HepG2 cells expressing microRNA miR-122 support the entire hepatitis C virus life cycle. *J Virol* **85**, 12087–12092.

Nakamuta, M., Fujino, T., Yada, R., Aoyagi, Y., Yasutake, K., Kohjima, M., Fukuizumi, K., Yoshimoto, T., Harada, N. & other authors (2011). Expression profiles of genes associated with viral entry in HCV-infected human liver. *J Med Virol* **83**, 921–927.

Nishimura, G., Ikeda, M., Mori, K., Nakazawa, T., Ariumi, Y., Dansako, H. & Kato, N. (2009). Replicons from genotype 1b HCV-positive sera exhibit diverse sensitivities to anti-HCV reagents. *Antiviral Res* **82**, 42–50.

Pietschmann, T., Lohmann, V., Kaul, A., Krieger, N., Rinck, G., Rutter, G., Strand, D. & Bartenschlager, R. (2002). Persistent and transient replication of full-length hepatitis C virus genomes in cell culture. *J Virol* **76**, 4008–4021.

Pietschmann, T., Zayas, M., Meuleman, P., Long, G., Appel, N., Koutsoudakis, G., Kallis, S., Leroux-Roels, G., Lohmann, V. & Bartenschlager, R. (2009). Production of infectious genotype 1b virus particles in cell culture and impairment by replication enhancing mutations. *PLoS Pathog* **5**, e1000475.

Sainz, B., Jr, Barretto, N., Martin, D. N., Hiraga, N., Imamura, M., Hussain, S., Marsh, K. A., Yu, X., Chayama, K. & other authors (2012).

Identification of the Niemann–Pick C1-like 1 cholesterol absorption receptor as a new hepatitis C virus entry factor. *Nat Med* **18**, 281–285.

Tanaka, T., Kato, N., Cho, M. J., Sugiyama, K. & Shimotohno, K. (1996). Structure of the 3′ terminus of the hepatitis C virus genome. *J Virol* **70**, 3307–3312.

Tellinghuisen, T. L., Foss, K. L. & Treadaway, J. (2008). Regulation of hepatitis C virion production via phosphorylation of the NS5A protein. *PLoS Pathog* **4**, e1000032.

Ueda, Y., Mori, K., Ariumi, Y., Ikeda, M. & Kato, N. (2011). Plural assay systems derived from different cell lines and hepatitis C virus strains are required for the objective evaluation of anti-hepatitis C virus reagents. *Biochem Biophys Res Commun* **409**, 663–668.

Wakita, T., Pietschmann, T., Kato, T., Date, T., Miyamoto, M., Zhao, Z., Murthy, K., Habermann, A., Kräusslich, H. G. & other authors (2005). Production of infectious hepatitis C virus in tissue culture from a cloned viral genome. *Nat Med* **11**, 791–796.

Zhong, J., Gastaminza, P., Cheng, G., Kapadia, S., Kato, T., Burton, D. R., Wieland, S. F., Uprichard, S. L., Wakita, T. & Chisari, F. V. (2005). Robust hepatitis C virus infection in vitro. *Proc Natl Acad Sci U S A* **102**, 9294–9299.

FEBS Open Bio 2 (2012) 279–283

ELSEVIER

FEBS openbio

journal homepage: www.elsevier.com/locate/febsopenbio

Raloxifene inhibits hepatitis C virus infection and replication

Midori Takeda[a,1], Masanori Ikeda[a,*,1], Kyoko Mori[a], Masahiko Yano[a], Yasuo Ariumi[a,2], Hiromichi Dansako[a], Takaji Wakita[b], Nobuyuki Kato[a]

[a] Department of Tumor Virology, Okayama University Graduate School of Medicine, Dentistry, and Pharmaceutical Sciences, Okayama 700-8558, Japan
[b] Department of Virology II, National Institute of Infectious Disease, Tokyo 162-8640, Japan

ARTICLE INFO

Article history:
Received 21 May 2012
Received in revised form 27 July 2012
Accepted 8 August 2012

Keywords:
Hepatitis C virus
Raloxifene
Estrogen
Osteoporosis
Statin

ABSTRACT

Postmenopausal women with chronic hepatitis C exhibited a poor response to interferon (IFN) therapy compared to premenopausal women. Osteoporosis is the typical complication that occurs in postmenopausal women. Recently, it was reported that an osteoporotic reagent, vitamin D3, exhibited anti-hepatitis C virus (HCV) activity. Therefore, we investigated whether or not another osteoporotic reagent, raloxifene, would exhibit anti-HCV activity in cell culture systems. Here, we demonstrated that raloxifene inhibited HCV RNA replication in genotype 1b and infection in genotype 2a. Raloxifene enhanced the anti-HCV activity of IFN-α. These results suggest a link between the molecular biology of osteoporosis and the HCV life cycle.

1. Introduction

Hepatitis C virus (HCV) belongs to the *Flaviviridae* family and contains a positive single-stranded RNA genome of 9.6 kb. The HCV genome encodes a single polyprotein precursor of approximately 3000 amino acid residues, which is cleaved by the host and viral proteases into at least 10 proteins in the following order: Core, envelope 1 (E1), E2, p7, nonstructural 2 (NS2), NS3, NS4A, NS4B, NS5A, and NS5B [1–3].

The virological study and screening of antiviral reagents for HCV was difficult until the replicon system was developed [4–7]. In 2005, an infectious HCV production system was developed using genotype 2a HCV JFH-1 and hepatoma-derived HuH-7 cells, and the HCV life cycle was reproduced in a cell culture system [8]. We previously developed genome-length HCV reporter assay systems using HuH-7-derived OR6 cells [4]. In OR6 cells, the genotype 1b HCV-O with renilla luciferase (*RL*) replicates robustly. We also developed an HCV JFH-1 reporter infection assay system [9].

HCV infection frequently causes chronic hepatitis (CH) and leads to serious liver cirrhosis and hepatocellular carcinoma. Therefore, HCV infection is a major health problem worldwide. The elimination of HCV by antiviral reagents seems to be the most efficient therapy for preventing the fatal state of the disease. Pegylated-interferon (PEG-IFN) with ribavirin (RBV) is the current standard therapy for CH–C, but its sustained virological response (SVR) rate has remained 40–50%. Recently, a protease inhibitor, telaprevir, improved the SVR rate by up to 60–70% in combination with PEG-IFN/RBV [10]. The response to PEG-IFN/RBV therapy depends on host factors as well as viral factors. Among the host factors, age and gender are known to be associated with the outcome of IFN/RBV therapy [11,12]. Postmenopausal women with CH–C exhibited a poor response to IFN therapy compared to premenopausal women [11]. The decrease in estrogen may affect the response to IFN therapy. Dyslipidemia and osteoporosis are the typical complications in postmenopausal women. We and other groups reported that statins, which are dyslipidemia reagents, inhibited HCV proliferation in vitro and in vivo [13–17]. Recently it was reported that vitamin D3, an osteoporotic reagent, exhibited anti-HCV activity in vitro and in vivo [18–21]. It was also reported that 17β-estradiol inhibited the production of infectious HCV [22]. Taken together, these reports suggest an association between hepatitis C and complications due to the decrease of estrogen.

Raloxifene and tamoxifen are synthetic selective estrogen receptor modulators (SERMs) and are used for breast cancer and osteoporosis, respectively, in clinical settings. The responses of SERMs are mediated by estrogen receptors (ERs), either ERα or ERβ. SERMs exhibit agonistic actions in some tissues but antagonistic actions in others. Both raloxifene and tamoxifen are antagonists in breast and agonists in bone. However, only tamoxifen, and not raloxifene, exhibited agonistic activity in the uterus. It was reported that tamoxifen inhibited HCV RNA replication [23]. However, tamoxifen's agonist action leads to uterine cancer. Raloxifene belongs to an antiosteoporotic reagent and offers the advantage of safety without uterine cancer. Therefore, we decided to investigate whether or not raloxifene would exhibit anti-HCV activity in our developed cell culture systems.

[1] These authors contributed equally to this work.
[2] Current address: Center for AIDS Research, Kumamoto University, Kumamoto 860-0811, Japan.
* Corresponding author. Fax: +81 86 235 7392.
E-mail address: maikeda@md.okayama-u.ac.jp (M. Ikeda).

2211-5463/$36.00
http://dx.doi.org/10.1016/j.fob.2012.08.003

2. Materials and methods

2.1. Reagents and antibodies

Raloxifene was purchased from LKT Laboratories, Inc. (St. Paul, MN). IFN-α and tamoxifen were purchased from Sigma–Aldrich (St. Louis, MO). Pitavastatin (PTV) was purchased from Kowa Company (Nagoya, Japan). The antibodies used in this study were those specific to HCV Core (CP11, Institute of Immunology, Tokyo, Japan), NS3 (Novocastra Laboratories, Newcastle, UK), and β-actin (Sigma).

2.2. Cell culture and HCV RNAs

HuH-7 cells were cultured in Dulbecco's modified Eagle's medium (Gibco-BRL, Invitrogen Life Technology, Carlsbad, CA) supplemented with 10% fetal bovine serum, penicillin, and streptomycin. HuH-7-derived OR6 and sOR cells were genome-length and subgenome HCV (O strain of genotype 1b) RNA harboring cells, respectively and cultured in the above medium supplemented with G418 (0.3 mg/ml; Geneticin, Invitrogen) [4]. HCVs replicating in OR6 and sOR cells contain *RL* and neomycin phosphotransferase (*NPT*) genes after 5′-untranslated region (UTR). HuH-7-derived RSc cells are cured cells, in which HCV RNA was eliminated by IFN-α; they are used for HCV JFH-1 infection [9]. RSc cells are also used for subgenomic JFH-1 RNA (JRN/35B) replication. JRN/35B contains *RL* and *NPT* genes after 5′-UTR.

2.3. RL assay

For the RL assay, 1.5×10^4 OR6 were plated onto 24-well plates in triplicate and cultured for 24 h. The cells were treated with each reagent for 72 h. Then the cells were harvested with *Renilla* lysis reagent (Promega, Madison, WI) and subjected to RL assay according to the manufacturer's protocol.

2.4. WST-1 cell proliferation assay

The cells (2×10^3 cells) were plated onto a 96-well plate in triplicate at 24 h before treatment with each reagent. At 72 h after treatment, the cells were subjected to a WST-1 cell proliferation assay (Takara Bio, Otsu, Japan) according to the manufacturer's protocol.

2.5. Western blot analysis

For Western blot analysis, 4×10^4 cells were plated onto 6-well plates, cultured for 24 h, and then treated with reagent(s) for 72 h and 120 h. Preparation of the cell lysates, sodium dodecyl sulfate–polyacrylamide gel electrophoresis, and immunoblotting were then performed as previously described [24]. Immunocomplexes on the membranes were detected by enhanced chemiluminescence assay (Renaissance; Perkin Elmer Life Science, Wellesley, MA).

2.6. HCV infection

RSc cells (1.5×10^4 cells) were plated onto a 24-well plate 24 h before infection. To evaluate the effect of the treatment prior to infection, the cells were first treated with raloxifene for 24 h, then inoculated with reporter JFH-1 (JR/C5B/BX-2) supernatant at a multiplicity of infection (MOI) of 0.2, cultured for 48 h, and subjected to RL assay as described previously [9]. The JR/C5B/BX-2 contains the *RL* gene in the first cistron following the encephalomyocarditis virus-internal ribosomal entry site (*EMCV-IRES*) gene and the open reading frame (ORF) of JFH-1 in the second cistron. To evaluate the effect of the treatment after infection, the cells were inoculated with reporter JFH-1 supernatant at MOI of 0.2, cultured for 72 h, and subjected to RL assay.

3. Results

3.1. Raloxifene inhibited HCV RNA replication

The HCV RNA that replicated in HuH-7-derived OR6 cells was a genome-length HCV with *RL*, *NPT*, and *EMCV-IRES* in the first cistron and the ORF of HCV (O strain of genotype 1b) in the second cistron [4]. OR6 cells could not produce infectious HCV. Therefore, we can monitor the replication step in the HCV life cycle using OR6 cells. Raloxifene inhibited HCV RNA replication in a dose-dependent manner, and its 50% effective concentration (EC_{50}) was 1 μM (Fig. 1A). Raloxifene did not exhibit cytotoxicity to OR6 cells until 2.5 μM (Fig. 1B). Raloxifene also inhibited intracellular Core and NS3 production in a dose- and time-dependent manner (Fig. 1C). The intensities of Core and NS3 in OR6 cells treated with 2.5 μM of raloxifene decreased to almost the level of cells treated with 10 IU/ml of IFN-α at 120 h after treatment. We also examined anti-HCV activity of raloxifene using subgenomic HCV replicon harboring sOR cells. Raloxifene exhibited weak anti HCV activity to sOR cells as compared with OR6 cells (Supplementary Figs. 1A and 1B). These results suggest that raloxifene exhibits anti-HCV activity and decreased the expression levels of HCV proteins more slowly compared to IFN-α.

3.2. Raloxifene enhanced anti-HCV activity of IFN-α

We investigated the anti-HCV activity of raloxifene in combination with a representative anti-HCV reagent, IFN-α. HCV RNA replication decreased in a dose-dependent manner after co-treatment with IFN-α and raloxifene (Fig. 2A). The results were almost similar to the expected effect of raloxifene in combination with IFN-α calculated from the anti-HCV activity of each reagent (Fig. 2B). These results indicate that the anti-HCV activity of raloxifene and IFN-α exhibited additive effect. We also examined the anti-HCV activity of previously reported SERM, tamoxifen. Tamoxifen also exhibited additive anti-HCV activity on HCV RNA replication in combination with IFN-α (Supplementary Figs. 2A–C). These results indicate that raloxifene as well as tamoxifen enhanced the anti-HCV activity of IFN-α. As both raloxifene and IFN-α are clinically used reagents, raloxifene seemed to be a candidate reagent as an add-on treatment to IFN-α in patients with CH–C.

3.3. Raloxifene antagonized anti-HCV activity of statin

We previously reported that statins exhibited anti-HCV activity using the OR6 assay system [14]. Statin is the first-choice reagent for dyslipidemia. As dyslipidemia and osteoporosis are major complications in postmenopausal women, we invested the effect of raloxifene on the anti-HCV activity of PTV. Raloxifene did not enhance the anti-HCV activity of PTV (Fig. 3A). Fig. 3B exhibits the expected anti-HCV activity of co-treatment with raloxifene and PTV calculated from the anti-HCV effect of either raloxifen or PTV alone. Raloxifene exhibited an antagonistic effect on PTV's anti-HCV activity. Raloxifene's antagonistic effect on PTV increased dose-dependently. The co-treatment with raloxifene (2.5 μM) and PTV (0.25, 0.5, and 1 μM) resulted in lower anti-HCV activity than did treatment with raloxifene alone (2.5 μM). These results suggest that we should be careful in the administration of statins with raloxifene to postmenopausal woman with CH–C.

3.4. Raloxifene inhibited infection of genotype 2a HCV

To further investigate the anti-HCV activity of raloxifene, we examined whether or not raloxifene could inhibit HCV infection. For this purpose, we used our recently developed JFH-1 reporter infection assay system [9]. HuH-7-derived RSc's are highly HCV-permissive cell lines. Raloxifene was pretreated at 24 h before HCV infection. The cells were inoculated with HCV JFH-1 virion with *RL* (JR/C5B/BX-2), and

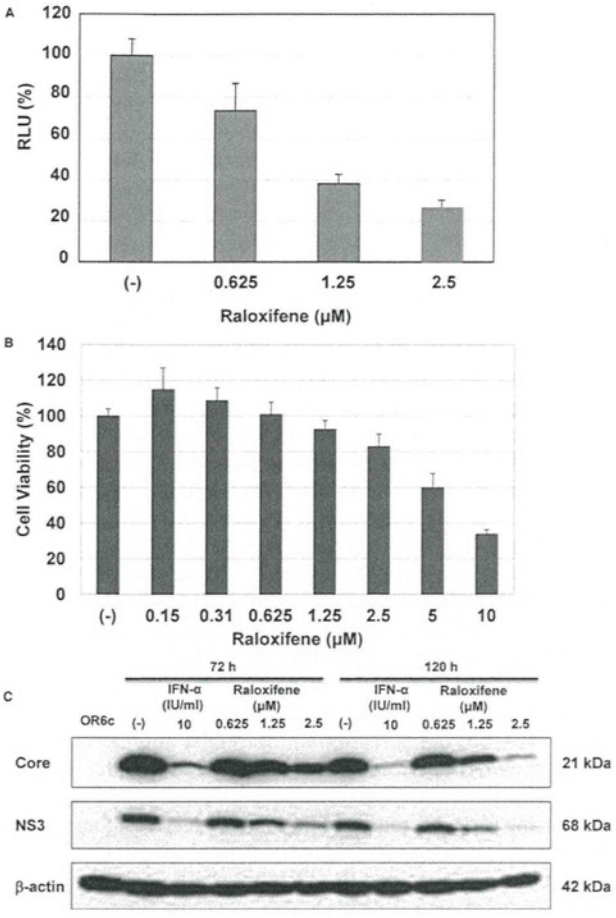

Fig. 1. Raloxifene inhibited HCV RNA replication. (A) Anti-HCV activity of raloxifene in OR6 cells. OR6 cells were treated with raloxifene (0, 0.625, 1.25, and 2.5 μM) for 72 h. Relative RL activity (relative light unit: RLU) for HCV RNA replication is expressed as a percentage of control. Each bar represents the average with standard deviations of triplicate data points. (B) Effect of raloxifene on OR6 cell viability. Cell viability at 72 h after raloxifene treatment (0.15, 0.31, 0.625, 1.25, 2.5, 5, and 10 μM) was determined using WST-1 cell proliferation assay and is expressed as a percentage of control. (C) Raloxifene inhibited HCV proteins. OR6 cells were treated with IFN-α (10 IU/ml) or raloxifene (0, 0.625, 1.25, and 2.5 μM). After 72 or 120 h treatment, the production of Core and that of NS3 were analyzed by immunoblotting using anti-Core and anti-NS3 antibodies, respectively. OR6c cells were cured cells in which HCV RNA was eliminated using IFN-α, and were used as a negative control. β-actin was used as a control for the amount of protein loaded per lane.

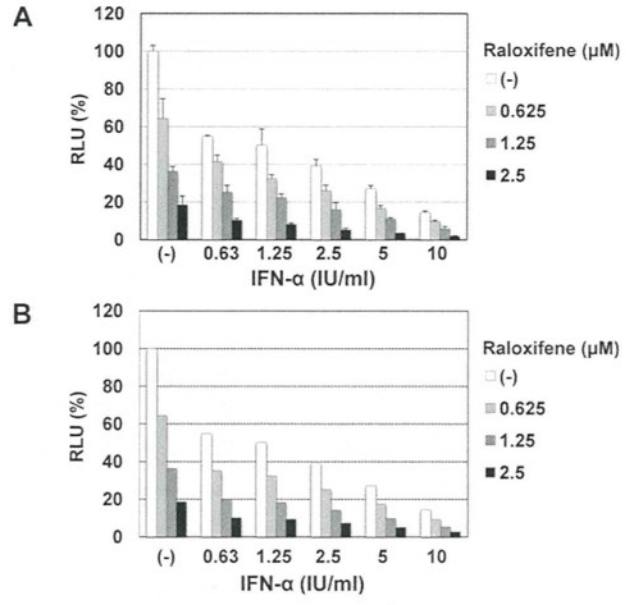

Fig. 2. Raloxifene enhanced the anti-HCV activity of IFN-α. (A) Anti-HCV activity of raloxifene in combination with IFN-α. OR6 cells were co-treated with raloxifene (0, 0.625, 1.25, and 2.5 μM) and IFN-α (0, 0.63, 1.25, 2.5, 5, 10 IU/ml). Relative RL activity is shown as a percentage of control. Each bar represents the average with standard deviations of triplicate data points. (B) Expected anti-HCV activity was calculated based on the results when the cells were treated with only raloxifene or IFN-α.

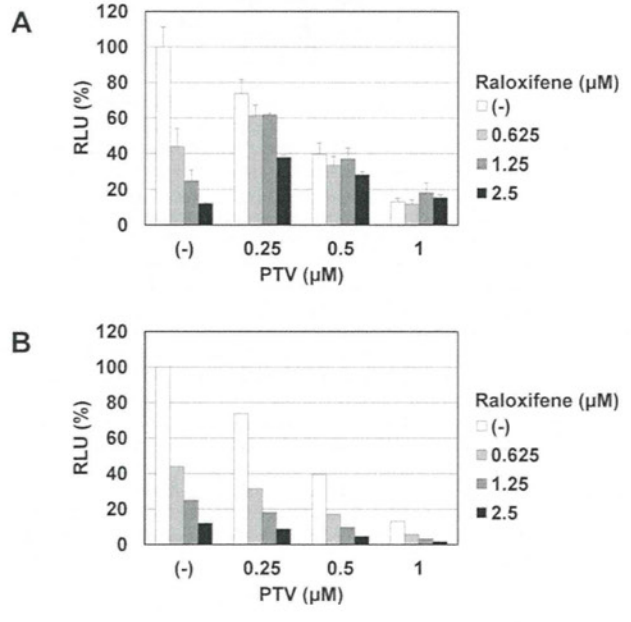

Fig. 3. Statin antagonized the anti-HCV activity of raloxifene. (A) OR6 cells were co-treated with raloxifene (0, 0.625, 1.25, and 2.5 μM) and PTV (0, 0.25, 0.5, and 1 μM). Relative RL activity was shown as a percentage of control. Each bar represents the average with standard deviations of triplicate data points. (B) Expected anti-HCV activity was calculated based on the results when the cells were treated with only raloxifene or PTV.

the infection was monitored with RL activity at 48 h after infection. As shown in Fig. 4A, raloxifene inhibited HCV infection in RSc cells in a dose-dependent manner. Next we examined the effect of raloxifene after HCV infection. RSc cells were inoculated with HCV JFH-1 virion with *RL*. After HCV infection, the cells were treated with raloxifene for 72 h and raloxifene's inhibitory effect on post-infection was assessed using the RL assay. Raloxifene inhibited HCV proliferation in a dose-dependent manner when it was added to the cells after infection in RSc cells, although inhibitory effect of raloxifene on JFH-1 HCV RNA replication seemed to be weak compared to the genotype 1b HCV-O RNA replication (Fig. 4B). Raloxifene did not exhibit cytotoxicity to RSc cells until 2.5 μM (Fig. 4C). We found that raloxifene could not inhibit subgenomic JFH-1 HCV (JRN/35B) RNA replication (Fig. 4D). We further examined the inhibitory action of raloxifene around infection step. RSc cells were treated for short time with raloxifene around infection step: for 1, 4, and 4 h before, during, and after inoculation, respectively (Fig. 4E). Raloxifene inhibited JFH-1 infection, when it was treated during inoculation but not just before or after inoculation. In case of genotype 2a JFH-1, raloxifene's anti-HCV activity is mainly due to the inhibition of infection. These results indicate that raloxifene inhibits JFH-1 infection but not its RNA replication.

4. Discussion

In this study, we demonstrated that raloxifene, an osteoporotic reagent, inhibited the replication of genotypes 1b HCV RNA replication and inhibited genotype 2a HCV JFH-1 infection. Raloxifene additively enhanced the anti-HCV activity of IFN-α. On the other hand, raloxifene exhibited an antagonistic effect on statins.

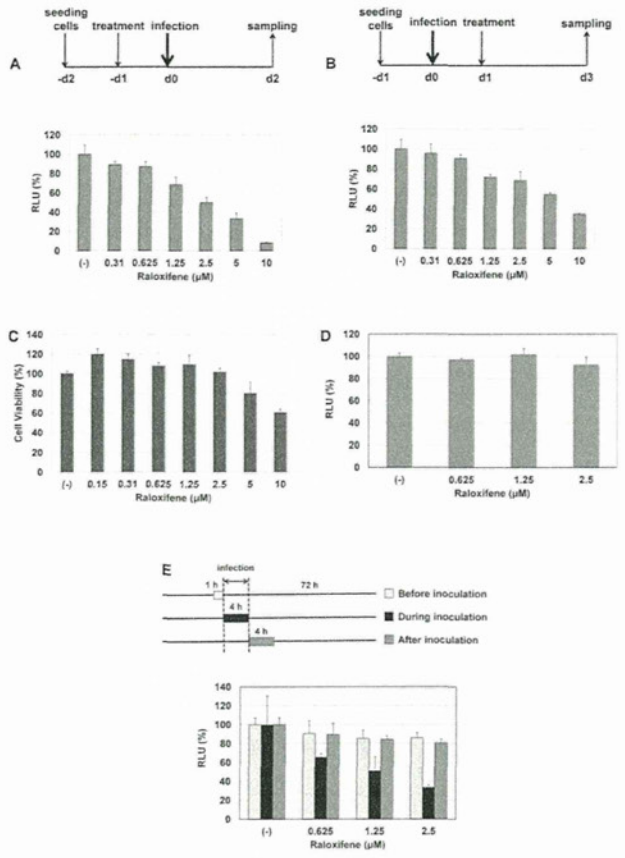

Fig. 4. Raloxifene inhibited genotype 2a HCV infection. (A) Raloxifene inhibited HCV JFH-1 infection. RSc cells were treated with raloxifene (0, 0.31, 0.625, 1.25, 2.5, 5, and 10 μM) 24 h before infection. HCV JFH-1 reporter virion was used as an inoculum after removal of raloxifene. The cells were then infected with reporter JFH-1 virion and cultured for 48 h. The inhibition of HCV infection was assessed by relative RL activity and expressed as a percentage of control. (B) Raloxifene inhibited HCV JFH-1 proliferation after infection. RSc cells were inoculated with HCV JFH-1 reporter virion and cultured for 24 h. Then the cells were treated with raloxifene (0, 0.31, 0.625, 1.25, 2.5, 5, and 10 μM) for 48 h. The inhibitory effect on HCV proliferation after infection was assessed by relative RL activity and expressed as a percentage of control. Each bar represents the average with standard deviations of triplicate data points. (C) Effect of raloxifene on RSc cells viability. Cell viability at 72 h after raloxifene treatment (0.15, 0.31, 0.625, 1.25, 2.5, 5, and 10 μM) was determined using WST-1 cell proliferation assay and is expressed as a percentage of control. (D) Subgenomic JFH-1 RNA (JRN/35B) replicating RSc cells were treated with raloxifene (0, 0.625, 1.25, and 2.5 μM) for 72 h. Relative RL activity for HCV RNA replication is expressed as a percentage of control. Each bar represents the average with standard deviations of triplicate data points. (E) Raloxifene (0, 0.625, 1.25, and 2.5 μM) was treated for 1, 4, and 4 h before, during, and after JFH-1 inoculation to RSc cells at MOI of 0.2, respectively. The cells were then cultured for 72 h. The inhibition of HCV infection was assessed by relative RL activity and expressed as a percentage of control.

PEG-IFN/RBV therapy led to a 40–50% SVR rate among patients with CH–C. Telaprevir with PEG-IFN/RBV increases the effect of PEG-IFN/RBV therapy by 10–20%. However, the major complication of anemia in PEG-IFN/RBV therapy increased when telaprevir was added. Considering that PEG-IFN/RBV-based therapy is less effective on postmenopausal women, an alternative therapy with minimal side effects is needed. Add-on therapy for postmenopausal women may be a candidate for improving the SVR in these patients. We focused on the reagents, which compensate for the lack of estrogen function. Dyslipidemia and osteoporosis are the major complications in postmenopausal women, and these complications are attributable to the decrease in estrogen. Statins are clinically used reagents for dyslipidemia; they inhibit HCV RNA replication in vivo as well as in vitro [13–17]. Therefore, we investigated whether or not raloxifene exhibits anti-HCV activity using genotype 1b HCV RNA replication and genotype 2a infection systems. In the HCV life cycle, raloxifene inhibited genotype 2a HCV infection and genotypes 1b HCV RNA replication. Raloxifene may be a potential reagent with different anti-HCV mechanisms in the HCV life cycle. Further study is needed to clarify these underlying mechanisms.

Recently it was reported that vitamin D3, an osteoporotic reagent, inhibited HCV production in cell culture systems [20,21]. Furthermore, it was reported that vitamin D3 was associated with the effect of therapy for patients with CH–C [18,19]. Statins inhibited HCV RNA replication by suppressing geranylgeranyl pyrophosphate (GGPP) production [14]. Another osteoporotic reagent, bisphosphonate, may possess anti-HCV activity, because it also inhibited the biosynthesis of GGPP in the mevalonate pathway by inhibiting farnesyl pyrophosphate synthetase. Taken together, these findings indicate it is likely that the HCV life cycle is associated with osteoporosis.

Raloxifene and tamoxifen are SERMs for osteoporosis and breast cancer, respectively. Tamoxifen is used for estrogen receptor-positive breast cancer, and it inhibits HCV RNA replication in cell culture [23]. Tamoxifen's anti-HCV activity is associated with ERα. In our study, raloxifene inhibited HCV infection as well as replication. To clarify the multi-potential effects of raloxifene, further study is needed. The incidence of side effects including uterine cancer is lower in raloxifene therapy than in tamoxifen therapy [25]. This is another advantage of raloxifene in clinical use for patients with CH–C.

As for the precise role of ERα or ERβ on the HCV life cycle, we could not reach a clear conclusion because microarray analysis revealed an absence of expression for both ERα and ERβ in OR6 cells (data not shown). Hayashida et al. [22] reported that the most potent physiological estrogen, 17-β-estradiol, inhibited infectious HCV production using HuH-7.5 cells, and that ERα-selective agonist inhibited infectious HCV production whereas ERβ-selective agonist did not. Watashi et al. [23] reported that RNA interference-mediated knockdown of ERα reduced HCV RNA replication. In our study, the anti-HCV activity of raloxifene in infection and replication did not seem attributable to ERα or ERβ. It is not clear why our HuH-7-derived OR6 cells did not express ERα or ERβ. HuH-7 cells were developed in 1982 at Okayama University and distributed worldwide [26]. Recently, Bensadoun et al. [27] reported that the genetic background of the IL28B genotype of HuH-7 cells differed among different laboratories. This may be a consequence of the polyploidal nature of hepatoma cells. A similar mechanism might cause the different expression levels of ERα and ERβ. Another ER, GPR30 [28], was expressed in OR6 cells (data not shown; from microarray analysis). GPR30 may be the responsible host factor for anti-HCV activity in OR6 cells. Further study is needed to clarify this issue.

In conclusion, we found that raloxifene inhibited HCV RNA replication in genotype 1b and infection in genotype 2a. Raloxifene additively enhanced the anti-HCV activity of IFN-α. The antagonistic effects of statins and raloxifene will yield information on the clinical use of these reagents. Our results, as well as the reports of vitamin D3's anti-HCV activity, will open new fields of treatment for both osteoporosis and HCV infection.

Acknowledgments

The authors would like to thank Masayo Takemoto for her technical assistance. This work was supported by a Grant-In-Aid for Research on Hepatitis from the Ministry of Health, Labor and Welfare of Japan.

Supplementary Material

Supplementary material associated with this article can be found, in the online version, at doi:10.1016/j.fob.2012.08.003.

References

[1] Kato N. (2001) Molecular virology of hepatitis C virus. Acta Med. Okayama. 55, 133–159.
[2] Kato N., Hijikata M., Ootsuyama Y., Nakagawa M., Ohkoshi S., Sugimura T. et al. (1990) Molecular cloning of the human hepatitis C virus genome from Japanese patients with non-A, non-B hepatitis. Proc. Natl. Acad. Sci. USA. 87, 9524–9528.
[3] Tanaka T., Kato N., Cho M.J., Sugiyama K., Shimotohno K. (1996) Structure of the 3' terminus of the hepatitis C virus genome. J. Virol. 70, 3307–3312.
[4] Ikeda M., Abe K., Dansako H., Nakamura T., Naka K., Kato N. (2005) Efficient replication of a full-length hepatitis C virus genome, strain O, in cell culture, and development of a luciferase reporter system. Biochem. Biophys. Res. Commun. 329, 1350–1359.
[5] Ikeda M., Yi M., Li K., Lemon S.M. (2002) Selectable subgenomic and genome-length dicistronic RNAs derived from an infectious molecular clone of the HCV-N strain of hepatitis C virus replicate efficiently in cultured Huh7 cells. J. Virol. 76, 2997–3006.
[6] Lohmann V., Korner F., Koch J., Herian U., Theilmann L., Bartenschlager R. (1999) Replication of subgenomic hepatitis C virus RNAs in a hepatoma cell line. Science. 285, 110–113.
[7] Pietschmann T., Lohmann V., Kaul A., Krieger N., Rinck G., Rutter G. et al. (2002) Persistent and transient replication of full-length hepatitis C virus genomes in cell culture. J. Virol. 76, 4008–4021.
[8] Wakita T. (2005) Production of infectious hepatitis C virus in tissue culture from a cloned viral genome. Nat. Med. 11, 791–796.
[9] Takeda M., Ikeda M., Ariumi Y., Wakita T., Kato N (2012) Development of hepatitis C virus production reporter assay systems using two different hepatoma cell lines. J. Gen. Virol. 93, 1422–1431.
[10] McHutchison J.G. (2009) Telaprevir with peginterferon and ribavirin for chronic HCV genotype 1 infection. N. Engl. J. Med. 360, 1827–1838.
[11] Hayashi J., Kishihara Y., Ueno K., Yamaji K., Kawakami Y., Furusyo N. et al. (1998) Age-related response to interferon alfa treatment in women vs men with chronic hepatitis C virus infection. Arch. Int. Med. 158, 177–181.
[12] Iwasaki Y. (2006) Limitation of combination therapy of interferon and ribavirin for older patients with chronic hepatitis C. Hepatology. 43, 54–63.
[13] Bader T., Fazili J., Madhoun M., Aston C., Hughes D., Rizvi S. et al. (2008) Fluvastatin inhibits hepatitis C replication in humans. Am. J. Gastroenterol. 103, 1383–1389.
[14] Ikeda M., Abe K., Yamada M., Dansako H., Naka K., Kato N. (2006) Different anti-HCV profiles of statins and their potential for combination therapy with interferon. Hepatology. 44, 117–125.
[15] Ikeda M., Kato N. (2007) Life style-related diseases of the digestive system: cell culture system for the screening of anti-hepatitis C virus (HCV) reagents: suppression of HCV replication by statins and synergistic action with interferon. J. Pharmacol. Sci. 105, 145–150.
[16] Rao G.A., Pandya P.K. (2011) Statin therapy improves sustained virologic response among diabetic patients with chronic hepatitis C. Gastroenterology. 140, 144–152.
[17] Sezaki H. (2009) An open pilot study exploring the efficacy of fluvastatin, pegylated interferon and ribavirin in patients with hepatitis C virus genotype 1b in high viral loads. Intervirology. 52, 43–48.
[18] Abu-Mouch S., Fireman Z., Jarchovsky J., Zeina A.R., Assy N. (2011) Vitamin D supplementation improves sustained virologic response in chronic hepatitis C (genotype 1)-naive patients. World J. Gastroenterol. 17, 5184–5190.
[19] Bitetto D. (2011) Vitamin D supplementation improves response to antiviral treatment for recurrent hepatitis C. Transpl. Int. 24, 43–50.
[20] Gal-Tanamy M., Bachmetov L., Ravid A., Koren R., Erman A., Tur-Kaspa R. et al. (2011) Vitamin D: an innate antiviral agent suppressing hepatitis C virus in human hepatocytes. Hepatology. 54, 1570–1579.
[21] Matsumura, T., Kato, T., Sugiyama, N., Tasaka-Fujita, M., Murayama, A., Masaki, T., Wakita, T., Imawari, M. 25-hydroxyvitamin D(3) suppresses hepatitis C virus production. Hepatology, in press.
[22] Hayashida K., Shoji I., Deng L., Jiang D.P., Ide Y.H., Hotta H. (2010) 17beta-estradiol inhibits the production of infectious particles of hepatitis C virus. Microbiol. Immunol. 54, 684–690.
[23] Watashi K., Inoue D., Hijikata M., Goto K., Aly H.H., Shimotohno K. (2007) Anti-hepatitis C virus activity of tamoxifen reveals the functional association of estrogen receptor with viral RNA polymerase NS5B. J. Biol. Chem. 282, 32765–32772.
[24] Kato N. (2003) Establishment of a hepatitis C virus subgenomic replicon derived from human hepatocytes infected in vitro. Biochem. Biophys. Res. Commun. 306, 756–766.
[25] Runowicz C.D., Costantino J.P., Wickerham D.L., Cecchini R.S., Cronin W.M., Ford L.G. et al. (2011) Gynecologic conditions in participants in the NSABP breast cancer prevention study of tamoxifen and raloxifene (STAR). Am. J. Obstet. Gynecol. 205, 535e1–535e5.
[26] Nakabayashi H., Taketa K., Miyano K., Yamane T., Sato J. (1982) Growth of human hepatoma cells lines with differentiated functions in chemically defined medium. Cancer Res. 42, 3858–3863.
[27] Bensadoun P., Rodriguez C., Soulier A., Higgs M., Chevaliez S., Pawlotsky J.M. (2011) Genetic background of hepatocyte cell lines: are in vitro hepatitis C virus research data reliable. Hepatology. 54, 748.
[28] Revankar C.M., Cimino D.F., Sklar L.A., Arterburn J.B., Prossnitz E.R. (2005) A transmembrane intracellular estrogen receptor mediates rapid cell signaling. Science. 307, 1625–1630.

Journal of Virology

Posttranslational Modification of Vesicular Stomatitis Virus Glycoprotein, but Not JNK Inhibition, Is the Antiviral Mechanism of SP600125

Sabrina Marozin, Jennifer Altomonte, Sibylle Apfel, Phat X. Dinh, Enrico N. De Toni, Antonia Rizzani, Andreas Nüssler, Nobuyuki Kato, Roland M. Schmid, Asit K. Pattnaik and Oliver Ebert

J. Virol. 2012, 86(9):4844. DOI: 10.1128/JVI.06649-11.
Published Ahead of Print 15 February 2012.

JVI
Journals.ASM.org

Posttranslational Modification of Vesicular Stomatitis Virus Glycoprotein, but Not JNK Inhibition, Is the Antiviral Mechanism of SP600125

Sabrina Marozin,[a] Jennifer Altomonte,[a] Sibylle Apfel,[a] Phat X. Dinh,[b] Enrico N. De Toni,[c] Antonia Rizzani,[c] Andreas Nüssler,[d] Nobuyuki Kato,[e] Roland M. Schmid,[a] Asit K. Pattnaik,[b] and Oliver Ebert[a]

Department of Medicine, Klinikum rechts der Isar, Technical University of Munich, Munich, Germany[a]; School of Veterinary Medicine and Biomedical Sciences and the Nebraska Center for Virology, University of Nebraska—Lincoln, Lincoln, Nebraska, USA[b]; Department of Medicine 2, University Hospital Grosshadern, University of Munich, Munich, Germany[c]; Department of Traumatology, Klinikum rechts der Isar, Technical University of Munich, Munich, Germany[d]; and Department of Molecular Biology, Okayama University Graduate School of Medicine, Dentistry, and Pharmaceutical Sciences, Okayama, Japan[e]

Vesicular stomatitis virus (VSV), a negative-sense single-stranded-RNA rhabdovirus, is an extremely promising oncolytic agent for cancer treatment. Since oncolytic virotherapy is moving closer to clinical application, potentially synergistic combinations of oncolytic viruses and molecularly targeted antitumor agents are becoming a meaningful strategy for cancer treatment. Mitogen-activated protein kinase (MAPK) inhibitors have been shown to impair liver cell proliferation and tumor development, suggesting their potential use as therapeutic agents for hepatocellular carcinoma (HCC). In this work, we show that the impairment of MAPK *in vitro* did not interfere with the oncolytic properties of VSV in HCC cell lines. Moreover, the administration of MAPK inhibitors did not restore the responsiveness of HCC cells to alpha/beta interferon (IFN-α/β). In contrast to previous reports, we show that JNK inhibition by the inhibitor SP600125 is not responsible for VSV attenuation in HCC cells and that this compound acts by causing a posttranslational modification of the viral glycoprotein.

Vesicular stomatitis virus (VSV), a negative-sense single-stranded-RNA rhabdovirus, which has inherent tumor specificity for replication due to attenuated type I interferon (IFN) (IFN-α/β) responses in most tumor cells, is an extremely promising oncolytic agent for cancer treatment (52, 53). A characterization of cellular events supporting VSV oncolysis is important for an understanding of virus-cell interactions in infected tumor cells, including hepatocellular carcinoma (HCC). Moreover, an investigation of the host cell determinants of permissiveness to VSV infection is essential for the development of viral vectors with enhanced oncolytic properties for HCC.

The c-Jun N-terminal kinases (JNKs) belong to the superfamily of mitogen-activated protein kinases (MAPKs), which also includes p38 MAPK and extracellular signal-regulated kinase (ERK) (57). MAPKs are usually involved in the regulation of cell proliferation, differentiation, and apoptosis (6, 28). JNKs are activated, together with p38 MAPK, by different stimuli, including stress factors, inflammatory cytokines, and cytotoxic and genotoxic factors and play a critical role in mediating apoptotic signaling (32). JNK and p38 MAPK signals are often deregulated during malignant transformation, and cancer cells can subvert these pathways to facilitate proliferation, survival, and invasion (4, 5, 17, 24). JNK has been reported to exert oncogenic functions in HCC, and an increased kinase activity correlates with increased tumor proliferation (8, 22). The inhibition of JNK has been shown to impair liver cell proliferation and tumor development, suggesting the potential use of these inhibitors as therapeutic agents for HCC (42).

Human HCC cells are highly resistant to tumor necrosis factor-related apoptosis-inducing ligand (TRAIL)-induced cytotoxicity (51). Interestingly, treatment with a JNK inhibitor (JNKi) (SP600125) sensitizes HCC cells to TRAIL, providing evidence that the activity of JNK is required for resistance to apoptosis in these tumors (41). Several members of different viral families activate JNK and p38 MAPK gene-regulated cascades, in some cases resulting in the induction of apoptosis in infected cells and increased viral replication (9, 18). In particular, the activation of the JNK transduction pathway has been observed during infection with several DNA and RNA viruses, suggesting an important role in viral replication (2, 7, 10, 19). Interestingly, JNK activation is a common feature of many disparate viruses; therefore, it may represent an important target for the development of antiviral treatments. The aberrant activation of JNK is an important feature of tumorigenesis, and the constitutive activation of JNK occurs in most HCCs. Since VSV is a promising therapeutic agent against HCC, here we were interested in investigating the role of JNK in VSV oncolysis. Our studies revealed that JNK inhibition by the inhibitor SP600125 does not play any role in the attenuation of VSV in HCC cells. Rather, this compound acts by inducing a posttranslational modification of the viral glycoprotein, resulting in a significant reduction in the infectivity of the virus in these cells.

MATERIALS AND METHODS

Cell lines, primary human hepatocytes, and viruses. Two human HCC cell lines (HepG2 and Huh-7), kind gifts from Ulrich Lauer (University Hospital of Tübingen), were maintained in Dulbecco's modified Eagle's medium (DMEM) supplemented with 10% fetal bovine serum (FBS), 1% L-glutamine (200 mM), 1% penicillin-streptomycin, 1% nonessential amino acids, and 1% sodium pyruvate. Immortalized human hepatocytes

Received 25 October 2011 **Accepted** 9 February 2012
Published ahead of print 15 February 2012
Address correspondence to Oliver Ebert, oliver.ebert@lrz.tum.de.

doi:10.1128/JVI.06649-11

(PH5CH8) were maintained in DMEM–F-12 medium. All cell cultures were regularly tested for mycoplasma contamination. Primary human hepatocytes (PHH) were derived from patients (negative for hepatitis B virus [HBV], hepatitis C virus [HCV], and HIV) who underwent surgical resections of liver tumors. Human hepatocytes were isolated by a two-step collagenase perfusion technique followed by Percoll gradient centrifugation for purification, as previously described (44). Wild-type VSV-green fluorescent protein (GFP) was generated as previously described (14). Virus stocks were produced on BHK-21 cells and stored at −80°C. Titers were determined by a plaque assay on BHK-21 cells (14).

Western blotting. Whole-cell extracts or isolated viral pellets were run on a 7.5% SDS-PAGE gel and transferred onto nitrocellulose membranes. Total cell lysates were prepared by using Cell Lysing buffer (Cell Signaling Technology Inc., Danvers, MA) containing a protease and phosphatase inhibitor cocktail. The protein concentration in the samples was determined by using a bicinchoninic acid (BCA) protein assay kit (Promega, Madison, WI) according to the manufacturer's instructions. After blocking for 1 h with 5% skim milk–Tris-buffered saline (TBS)–Tween, membranes were blotted with the following primary antibodies (Abs) overnight at 4°C: antibodies against basal and phosphorylated forms of JNK, ERK1 and -2, and p38 MAPK (Cell Signaling); VSV-G (Abcam, Cambridge, United Kingdom); and actin (Sigma-Aldrich, Munich, Germany) and anti-VSV serum (kindly provided by Douglas Lyles). After secondary staining with anti-rabbit or anti-mouse peroxidase-conjugated Abs (Jackson ImmunoResearch Laboratories Inc., West Grove, PA), protein bands were visualized on Amersham Hyper-Max film with the ECL chemiluminescence kit as recommended by the manufacturer (Amersham, Buckinghamshire, United Kingdom).

Viral growth assays. Single infections and one-step growth curves of recombinant VSV (rVSV)-GFP were performed on PHH, immortalized human hepatocytes (PH5CH8), and the HepG2 and Huh-7 cell lines. Cells were infected at a multiplicity of infection (MOI) of 0.1 or 10 according to the experiment. After adsorption for 1 h, the monolayers were washed three times with phosphate-buffered saline (PBS), and fresh medium was added. Aliquots of culture media were collected at the indicated times postinfection. Viral titers were determined by 50% tissue culture infective dose ($TCID_{50}$) analysis and represent the averages of data from triplicate experiments. For interferon protection assays, cells were mock treated or incubated with 1,000 IU/ml of universal type I IFN (PBL Biomedical Laboratories) overnight and subsequently infected with rVSV-GFP for 16 h.

Treatment with MAPK inhibitors, DTT, and urea. Cells were seeded at 80 to 90% confluence in 24-well plates overnight. The next morning, the culture media were replaced with fresh media containing dimethyl sulfoxide (DMSO) or MAPK inhibitors at the indicated concentrations. After pretreatment for 16 h, virus infections were carried out in the presence of freshly added inhibitors. Chemicals (SB203580 [10 μM], SP600125 [25 μM], and U0126 [10 μM]) were purchased from Calbiochem-Merck (Gibbstown, NJ). For experiments with the JNK inhibitor, Huh-7 cells were pretreated with SP600125 (25 μM), and infection was allowed to proceed either in the absence or in the presence of fresh inhibitor for the entire duration of the experiment. Viral titers were determined at 24 h postinfection (hpi) by $TCID_{50}$ analysis.

Dithiothreitol (DTT) was added to semipurified virions to final concentrations of 10 and 50 mM. Samples were incubated at 56°C for 15 min. Treatment with urea was performed by the incubation of virions with 8 M urea for 10 min at room temperature (RT); direct separation on SDS-PAGE gels was applied without preheating the samples.

For the chemical cross-linking of VSV, samples of semipurified virions were incubated with SP600125 to a final concentration of 25 μM for 1 h on ice. Alternatively, cross-linking with 2% paraformaldehyde (PFA) was carried out on ice for 15 min. Samples were preheated at 56°C for 10 min and assayed by Western blotting.

Real-time PCR. Cells were infected with rVSV-GFP; cell supernatants and cell lysates were collected at the indicated time points. Cell debris was eliminated by centrifugation and total RNA was extracted, according to the manufacturers' instructions, by using the High Pure viral RNA kit (Roche, Mannheim, Germany) and the RNeasy Plus minikit (Qiagen, Valencia, CA), respectively. The forward and reverse primers generating a 138-nucleotide DNA fragment spanning one intergenic region between the N and P genes were designed as previously reported (14). Quantitative real-time PCR was carried out with the QuantiTect Probe reverse transcription kit (Qiagen, Valencia, CA) and the Kapa SYBR Fast qPCR Fast LightCycler 480 kit (PeqLab, Erlangen, Germany), using 15 ng of the template. The relative values for mRNA extracted from cell lysates were quantified by normalizing the expression level of the gene of interest to the level of the internal housekeeping control RNA (glyceraldehyde-3-phosphate dehydrogenase [GAPDH]). The quantification of viral RNA from infected supernatants was performed by using an external standard curve.

siRNA assays. For small interfering RNA (siRNA) experiments, reverse transfection was performed by using Lipofectamine RNAiMax (Invitrogen). Cells in 24-well plates were transfected with either 100 nM scrambled siRNA or specific siRNA (100 nM) according to the manufacturer's instructions. siRNAs were synthesized by Dharmacon (Thermo Fisher Scientific). After 48 to 72 h posttransfection, cultures were infected with rVSV-GFP at an MOI of 0.1 for 16 h. Titers were determined as the $TCID_{50}$. Cell lysates from uninfected duplicate cultures were analyzed by Western blotting to assess the efficiency of RNA silencing against JNK expression. Alternatively, 48 h after siRNA transfection, cells were treated with SP600125 or with DMSO and subsequently infected with VSV at an MOI of 0.1.

Transfection of a VSV glycoprotein-encoding plasmid and evaluation of syncytium formation. The VSV-G expression plasmid (pCMV-VSV-G) was kindly provided by Dorothee von Laer, Innsbruck, Austria. One microgram of plasmid was transfected into Huh-7 cells by using Lipofectamine LTX according to the manufacturer's instructions (Invitrogen). At 8 h posttransfection, the supernatant was replaced with fresh medium containing DMSO or SP600125 (25 μM). GFP under the control of a cytomegalovirus (CMV) promoter (pCMV-C3) was used as the transfection control. The presence of SP600125 did not influence transfection efficiency rates, as observed by the level of GFP expression and the number of GFP-positive cells with or without the inhibitor. Cell-cell fusion was allowed to progress without low-pH treatment to activate fusion, as previously described (11, 48).

After 24 to 36 h, cells were fixed with ice-cold 70% ethanol for 5 to 10 min at −20°C, and nuclei were visualized by propidium iodide staining. Syncytium formation was determined by the syncytium index (SI), calculated as the number of nuclei per syncytium divided by the number of nuclei per field of view. ImageJ software (National Institutes of Health, Bethesda, MD) was used to quantify the number of nuclei.

Glycosylation analysis. Semipurified virions obtained from DMSO- or SP600125-treated cells were subjected to digestion with endoglycosidase F (PNGase F) or with endo-α-*N*-acetylgalactosaminidase (EndoGalNAcase) (New England BioLabs, Frankfurt am Main, Germany). Samples were incubated overnight at 37°C, according to the manufacturer's instructions. Negative-control experiments were performed with deglycosylation buffers in the absence of the respective deglycosylation enzymes.

Mass spectrometry of the modified VSV G protein. Purified VSV obtained from SP600125-treated cells was separated on an SDS-PAGE gel. Viral proteins were stained with the Coomassie staining method, using GelCode Blue Stain reagent (Thermo Scientific) according to the manufacturer's instructions. Selected bands were excised and subjected to liquid chromatography (LC)/mass spectrometry (MS) as described previously (26). Briefly, gel pieces were digested with trypsin (catalog no. V5111; Promega, Madison, WI), and the digested peptides were extracted in 5% formic acid–50% acetonitrile and separated by using a C_{18} reversed-phase LC column (Milford, MA). A Q-TOF Ultima tandem mass spectrometer coupled with a Nanoaquity high-performance liquid chromatography (HPLC) system (Waters) with electrospray ionization was used to analyze the eluting peptides. The peak lists of tandem mass spectrom-

etry (MS/MS) data were generated by using Distiller (Matrix Science, London, United Kingdom), using charge state recognition and deisotoping with the other default parameters for Q-TOF data. Database searches of the acquired MS/MS spectra using NCBI database 20100701 were performed with Mascot (v2.2.0; Matrix Science, London, United Kingdom). Mass accuracy settings were 0.15 Da for peptide masses and 0.12 Da for fragment ion masses.

Statistical analysis. Data were analyzed for statistical significance by using GraphPad Prism 5.0 (GraphPad Software, San Diego, CA). Individual data points were compared by applying a two-sided Student *t* test, and *P* values of less than 0.05 were considered statistically significant.

RESULTS

JNK, ERK, and p38 MAPK activation in malignant and nonneoplastic hepatocytes infected with VSV. To examine the activation states of JNK, ERK, and p38 MAPK upon VSV infection, HCC cells (HepG2 and Huh-7), nonneoplastic immortalized hepatocytes (PH5CH8), and primary human hepatocytes (PHH) were infected with rVSV-GFP, and lysates were collected at different hours postinfection. The activation of these molecules occurs as a result of phosphorylation; therefore, the cell lysates were analyzed by Western blotting using phospho-specific antibodies to each of these proteins. JNK activation levels increased over time and peaked at different time points, depending on the cell type (Fig. 1A). In Huh-7 cells, the level of JNK activation was at its highest at 6 hpi and remained high until 12 hpi. In HepG2 and PH5CH8 cells, we observed a gradual increase of the level of the phosphorylated JNK form up to 12 hpi. However, in PHH, JNK activation was not significant, and only a slight increase at the final time point was detected. The levels of phosphorylated ERK in HCC cell lines showed a minimal increment at around 4 to 6 hpi but remained unchanged (in Huh-7 cells) or decreased at later time points. In contrast, p38 MAPK showed a delayed activation, occurring at 12 hpi. In HCC cells, the phosphorylation of JNK is a fairly late event during VSV infection, which starts at around 4 hpi, coincident with VSV glycoprotein (VSV-G) expression. Infection with a UV-inactivated virus did not induce JNK activation (data not shown).

To determine if JNK activity is necessary for the efficient replication of VSV in cell cultures, the effect of the JNK inhibitor (JNKi) SP600125 was compared to those of the ERK inhibitor (ERKi) and the p38 MAPK inhibitor (p38i). First, cells were pretreated with various chemical inhibitors and, in the presence of fresh inhibitors, infected with rVSV-GFP. VSV growth was significantly reduced only in the presence of JNKi, and attenuation was observed for all cell types (Fig. 1B). Western blotting for phospho-JNK indicated that the JNK inhibitor specifically reduced JNK phosphorylation in VSV-infected HCC cells without interfering with ERK activation (data not shown). In PHH, the inhibitory effect was not as pronounced, and additionally, ERK appeared to be affected. Nevertheless, ERK dephosphorylation was already present in VSV-infected cultures not treated with the JNK inhibitor. Thus, our results show that in contrast to JNK, the inhibition of ERK and p38 MAPK by their specific inhibitors did not influence VSV replication.

In addition, an siRNA-mediated knockdown of JNK was performed in HCC cell lines and nonneoplastic hepatocytes to confirm the specificity of SP600125. Cells were transfected with scramble (Scr) siRNA or a pool of two different siRNAs against JNK kinases, followed by infection with rVSV-GFP. Despite a robust decrease of JNK protein levels, viral replication was not affected, and no significant differences in titers were observed (Fig. 1C, left). To further define whether the inhibition of JNK was associated with the SP600125-dependent attenuation of VSV growth, HCC cells (data for HepG2 cells are shown) were transfected with either scramble or JNK-specific siRNAs (Fig. 1C, right). Infection was carried out in the absence or presence of SP600125, and viral titers were determined 24 h later. The effective knockdown of the JNK protein was assessed by Western blotting. As shown in Fig. 1C (right), in the presence of the JNK inhibitor, both scramble siRNA- and JNK siRNA-transfected cells were equally susceptible to SP600125, supporting the observation that productive VSV infection does not require JNK.

Inhibitors of the MAPK signal do not sensitize HCC cells to type I interferon. To determine the effect of the MAPK inhibitors on type I IFN sensitivity, cells were treated with ERK, p38 MAPK, and JNK inhibitors alone or in combination with IFN-α/β, followed by VSV infection, as described above. In all cell types, the viral titers were appreciably lower in cultures treated with the JNK inhibitor than in cultures treated with DMSO. A robust attenuation of virion production upon combined treatment with SP600125 and IFN-α/β was observed, especially in PHH and in PH5CH8 cells, indicating an additive effect of type I IFN with SP600125 activity on viral replication (Fig. 2A). The inhibition of ERK and p38 MAPK did not enhance the efficacy of IFN-α/β against VSV in HCC cells (Fig. 2B and C).

SP600125 can synergistically enhance cell apoptosis in cancer cells (30, 37, 41). We excluded apoptosis as the cause of VSV growth attenuation by SP600125, since the caspase inhibitor benzyloxycarbonyl-Val-Ala-Asp(OMe)-fluoromethylketone (Z-VAD-FMK) did not block the JNK inhibitor effect on viral titers, and SP600125 did not induced apoptosis in PHH (data not shown).

Viral transcription/translation and viral budding are not altered by SP600125. To identify the specific viral process blocked by the JNK inhibitor, we examined the levels of viral RNA transcription in cells treated with SP600125. HepG2 cells as well as PHH were pretreated with DMSO or SP600125 (25 μM) and infected with VSV at an MOI of 1. Total RNAs from cell lysates were harvested at different time points (0, 2, 4, and 8 hpi) and analyzed for the presence and concentrations of genomic VSV RNA and for nucleoprotein (N) mRNA by real-time PCR. The results show that the inhibition of JNK did not interfere with VSV mRNA transcription (Fig. 3A) or genome replication in HCC or in PHH cells (Fig. 3B). Additionally, levels of the VSV G protein in SP600125-treated cells were comparable to those in control samples (Fig. 3C). Furthermore, we compared the numbers of infectious viral particles in the lysates and in the supernatants of cells treated with vehicle (DMSO), interferon (IFN), or SP600125 (JNKi). In HCC cells treated with SP600125, the numbers of infectious particles in the cell lysates were comparable to that present in the corresponding supernatants (Fig. 3D).

Virions from cells treated with SP600125 are impaired in their infectivity. Since JNKi-treated cells produced significantly reduced titers of infectious virus, we next wanted to examine the molecular basis of this defect. HCC cells were mock treated or exposed to SP600125 or IFN-α/β overnight, followed by infection with rVSV-GFP. Viral titers as well as the RNA copy numbers in infected supernatants were measured. The number of budded viral particles was extrapolated by real-time PCR through the quantification of genomic viral RNA and compared to the correspond-

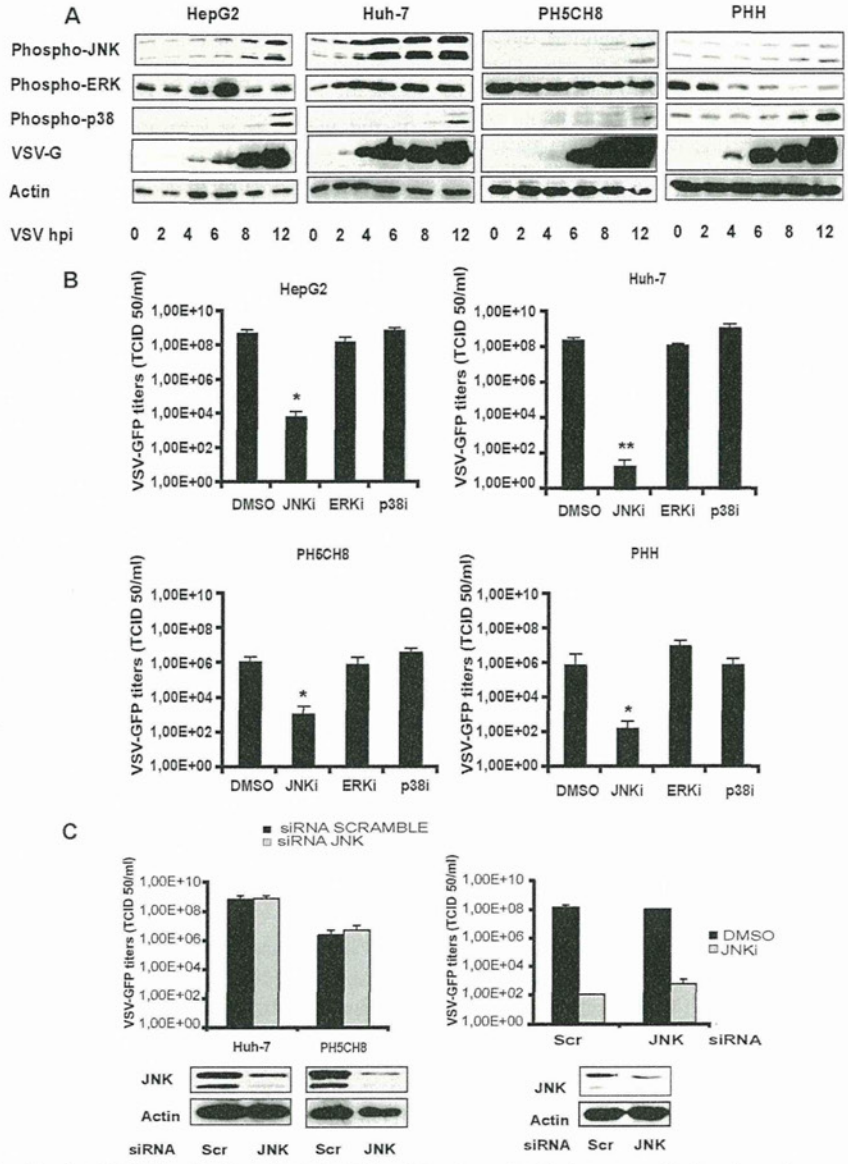

FIG 1 Activation of MAPK signaling in VSV-infected cells. (A) HCC cell lines (HepG2 and Huh-7), nonneoplastic primary hepatocytes (PH5CH8), and primary human hepatocytes (PHH) were infected with rVSV-GFP at an MOI of 10. The activation of JNK, ERK, and p38 MAPK was monitored at different time points postinfection by Western blotting via the detection of phosphorylated forms of the indicated kinases. (B) HCC cells, PH5CH8 cells, and PHH were mock treated (DMSO) or treated with SP600125 (JNKi) (25 μM), U0126 (ERKi) (10 μM), or SB203580 (p38i) and then infected with wild-type VSV at an MOI of 0.1 for 16 h. Error bars indicate standard deviations of data from experiments performed in triplicates. For all cell types, a statistically significant decrease of viral titers in SP600125-treated cells was observed (*, $P < 0.05$; **, $P < 0.01$). (C) HCC cells (data for Huh-7 cells are shown as representative data) and PH5CH8 cells were transfected with scramble siRNA (Scr) or JNK-specific siRNA. (Left) At 72 h posttransfection, cells were infected with wild-type VSV at an MOI of 0.1 for 16 h, and viral titers in the culture supernatants were determined by $TCID_{50}$ analysis. To confirm the siRNA knockdown, cell lysates of parallel uninfected cultures were subjected to Western blot analysis using an antibody specific for JNK. (Right) HepG2 cells transfected with scramble or JNK siRNAs were either left untreated or treated with SP600125 (25 μM) prior to VSV infection at an MOI of 0.1. Cell supernatants were assayed for viral yields, and total lysates were subjected to Western blotting for JNK expression.

ing infectious viral titers in the same supernatants (Fig. 4A). Numbers of copies of the VSV genome were slightly reduced upon treatment with SP600125. In contrast, IFN-α/β treatment also resulted in an inhibition of viral genome replication. While VSV titers in mock- and IFN-treated cells closely reflected the genome copy numbers, the number of infectious particles was significantly lower than the viral genome copy numbers in the supernatants of cells treated with SP600125, indicating that the JNKi may have affected virus infectivity without adversely affecting overall virion production. To determine if the loss of infectivity is due to reduced levels of incorporation of the viral proteins into budded virions, we examined the viral proteins in the culture supernatants of infected cells. Partially purified VSV from equal amounts of culture supernatants was pelleted, and levels of viral proteins in the viral pellets were analyzed by Western blotting. For cells treated with IFN-α/β, the levels of all viral proteins in the pellet were lower than those for mock-treated cells, consistent with the observed reduction in viral titers. Interestingly, in virus pellets

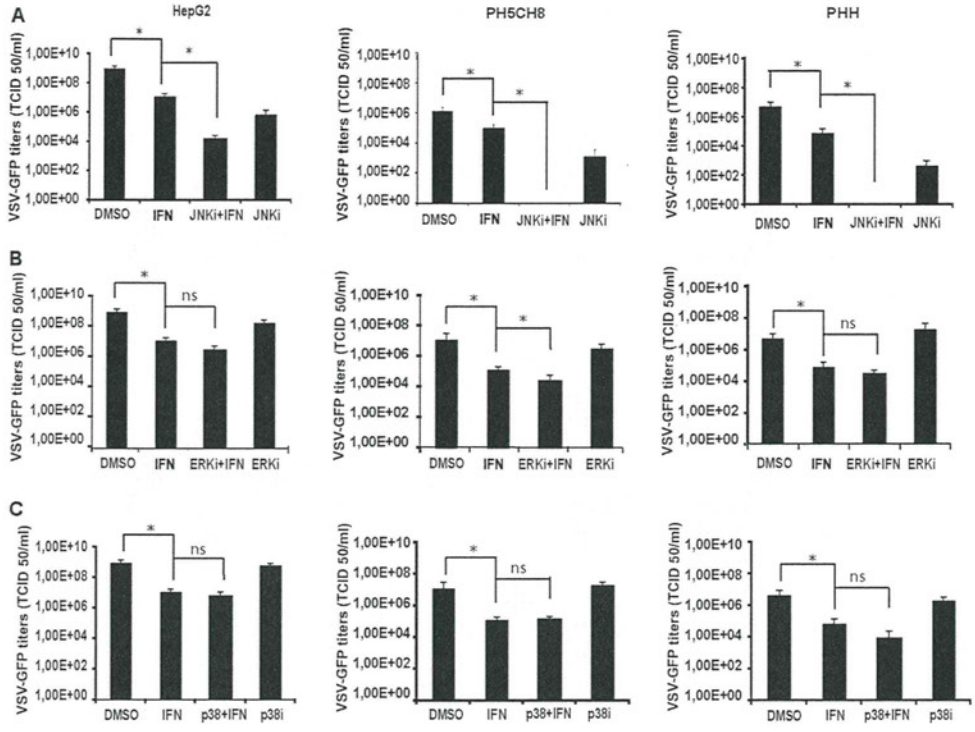

FIG 2 Antiviral activity of type I IFN in combination with MAPK inhibitors. HCC (data for HepG2 cells are shown as representative data), PH5CH8, and PHH cells were treated with IFN-α/β (100 IU/ml) in combination with 25 μM SP600125 (JNKi) (A), 10 μM U0126 (ERKi) (B), and 10 μM SB203580 (p38i) (C). Treatments with single agents and DMSO were included as controls. Infection with VSV-GFP at an MOI of 0.1 was then performed for 16 h, and viral titers were determined by $TCID_{50}$ analysis. Means of data from triplicate experiments are presented, with error bars indicating the standard deviations. Significance was determined by comparison with titers of control cultures (DMSO). *, $P < 0.05$; ns, nonsignificant.

from SP600125-treated cells, despite a significant reduction in VSV titers, the amount of VSV proteins was comparable to or higher than the levels in control cells (Fig. 4B). This result indicates that the loss of infectivity was not due to reduced levels of incorporation of viral G or other proteins into the budded virions. Most interestingly, the protein profile of virions produced from cells treated with SP60025 revealed an additional major protein band (identified as VSV-G*) of approximately 120 kDa, which appears to be related to the G protein (see below).

Moreover, to determine if the reduction of VSV growth in cells treated with the JNK inhibitor was due merely to differences in viral growth kinetics and, in particular, to a delay in particle release, we performed growth kinetics analyses. HCC cells were infected with VSV in the presence of vehicle (DMSO) or SP600125. Viral titers in the supernatants were determined at various times postinfection. A reduction of VSV replication in the presence of SP600125 was clearly observed during the entire duration of the kinetic analysis (Fig. 4C).

SP600125 alters VSV-G posttranslationally and hampers its fusogenic activity. As briefly described above, the purified virions and cell lysates from infected cells produced a slower-migrating band of about 120 kDa (VSV-G*), in addition to the normal G protein band, which appeared consistently when SP600125 was applied to the cells (Fig. 5A). This slower-migrating protein band was detected in infected cells or culture supernatants only in the presence of SP600125. As this additional band was specifically recognized by the antibody against VSV-G, we considered that it might represent a modified form of viral glycoprotein G. Additionally, this modified protein (VSV-G*) was also incorporated into the virions (Fig. 5A). Further studies revealed that the ectopic expression of the G protein in plasmid-transfected cells in the presence of JNKi also resulted in the appearance of this higher-molecular-weight protein band (Fig. 5B), indicating that the presence of the inhibitor may be responsible for the appearance of VSV-G* in virus-infected or plasmid-transfected cells. The sizes and levels of the other viral proteins were similar in untreated and SP600125-treated supernatants (Fig. 5C), indicating that SP600125 specifically induced the formation of this modified G protein. The anti-VSV antibody used in this experiment also detected the additional high-molecular-weight band. The presumptive modified viral glycoprotein (VSV-G*) was further analyzed by mass spectrometry. The fragments obtained after limited proteolysis could be identified as VSV-G protein peptides; no cellular proteins were consistently identified in VSV-G* preparations from two independent experiments (Table 1).

The effects of different reducing and denaturing agents were tested in an attempt to determine the nature of VSV-G*. Initially, we treated VSV-G* with dithiothreitol (DTT), a strong reducing agent, to assess the possible role of a disulfide bond in VSV-G* stability. Semipurified viral particles obtained from SP600125-treated cells were exposed to DTT prior to analysis by SDS-PAGE. Compared to samples treated with classical Laemmli buffer, containing 5% beta-mercaptoethanol and 2% SDS, DTT did not alter the stability or mobility of VSV-G* (Fig. 5D, left). Aliquots of lysates were then incubated at a different acidic pH and incubated at 4°C or preheated for 10 min at 65°C or 96°C. VSV-G* expres-

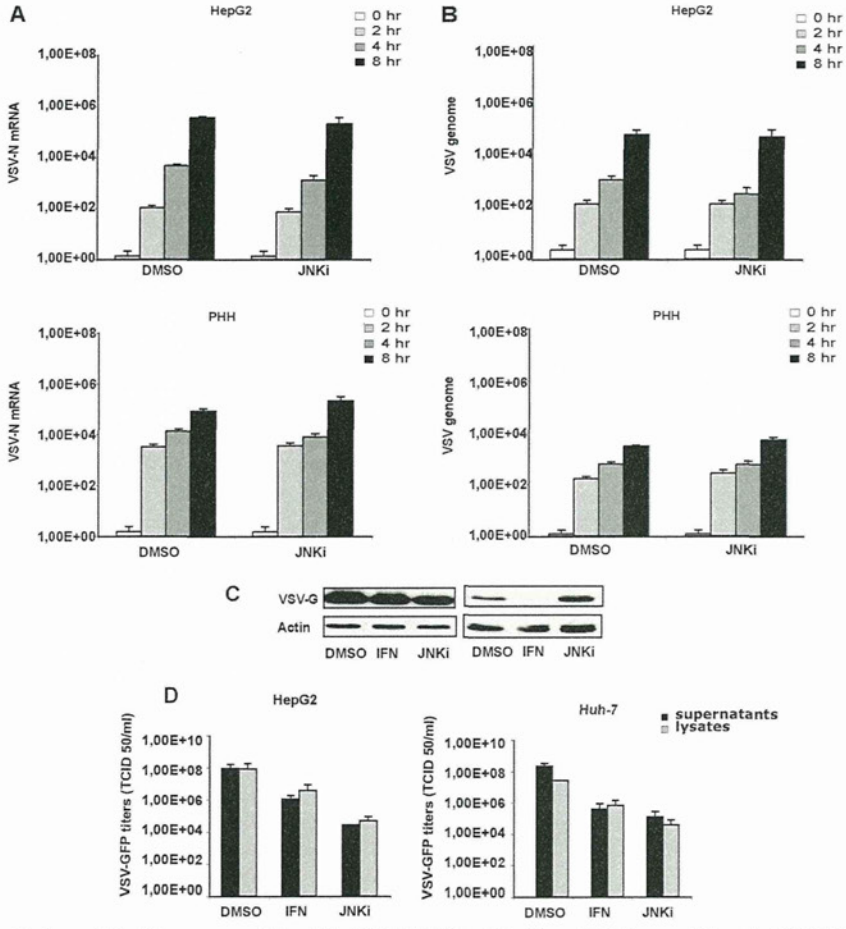

FIG 3 Viral transcription/translation and budding are not affected by SP600125. HepG2 cells and PHH were infected with VSV-GFP, and RNA was extracted at the indicated time points. (A and B) Viral mRNA for the N protein (A) and genome RNA (B) were quantified by real-time PCR. Data represent the means of data from three independent experiments. (C) Expression levels of VSV-G obtained from infected HepG2 cells and PHH previously treated with SP600125 (JNKi) or interferon (IFN) or left untreated were analyzed by Western blotting. (D) HCC cells left untreated (DMSO) or treated with SP600125 (JNKi) or IFN were infected with VSV-GFP for 16 h. Viral titers in the supernatants and corresponding cell lysates were quantified by $TCID_{50}$ analysis. Results represent the means of data from three independent experiments performed in duplicates.

sion was not affected by any of these treatments (data not shown). Additionally, to test a potential role of strong hydrophobic interactions in the VSV-G modification, the sensitivity of VSV-G* to urea treatment was analyzed. The exposure of SP600125-derived virions to 8 M urea did not affect the expression levels of both VSV-G and VSV-G*, as shown by Western blotting (Fig. 5D, right).

To exclude the possibility that SP600125 has the potential to cross-link the VSV glycoprotein, semipurified virions obtained from untreated cells were subjected either to direct exposure to SP600125 or to paraformaldehyde (PFA) (Fig. 6A). Samples were resolved by SDS-PAGE and detected by immunoblotting using an anti-VSV-G antibody. As shown in Fig. 6A, VSV-G could be cross-linked into species migrating at the molecular weight expected for dimeric and trimeric forms of the glycoprotein only upon treatment with PFA. This resulted in a drastic reduction in virus infectivity. However, the virions incubated with SP600125 retained their infectivity. Furthermore, when cells underwent pretreatment with only SP600125 and viral infection was allowed to proceed in the absence of the inhibitor, VSV growth was rescued. VSV-G* was still detectable in the corresponding cell lysates but at much lower expression levels than in control samples, where infection was carried out in the constant presence of the inhibitor (Fig. 6B).

Alterations of envelope glycosylation were shown previously to lead to impaired virus infectivity (58). To test the hypothesis that VSV-G* could be a hyperglycosylated form of wild-type VSV-G, we subjected semipurified virions to PNGase F or to EndoGalNAcase digestion, and we monitored the effect by Western blot analysis. PNGase F cleaves *N*-oligosaccharides from the glycoprotein, and EndoGalNAcase releases O-linked glycans instead. Both VSV-G and VSV-G* were susceptible to PNGase F digestion, which resulted in a shift to lower-molecular-weight proteins (Fig. 6C, left), whereas EndoGalNAcase had no effect on both protein species despite the extended incubation time (Fig. 6C, right). Notably, the enzyme treatments failed to shift VSV-G* to the fully deglycosylated form.

To determine if VSV-G* could compromise the functionality of the viral glycoprotein reducing infectivity of the virions, we assessed the ability of transfected VSV-G to induce syncytia in the presence of SP600125. Huh-7 cells were transfected with a plasmid encoding the VSV G protein, and at 8 h posttransfection,